





Atlas of Normal Microanatomy, Procedural and Processing Artifacts, Common Background Findings, and Neurotoxic Lesions in the Peripheral Nervous System of Laboratory Animals

Toxicologic Pathology
1-27
© The Author(s) 2019
Article reuse guidelines:
sagepub.com/journals-permissions
DOI: 10.1177/0192623319867322
journals.sagepub.com/home/tpx


Ingrid D. Pardo¹, Klaus Weber², Sarah Cramer³, Georg J. Krinke[†],
Mark T. Butt³, Alok K. Sharma⁴, and Brad Bolon⁵

Abstract

The ability to differentiate among normal structures, procedural and processing artifacts, spontaneous background changes, and test article-related effects in the peripheral nervous system (PNS) is essential for interpreting microscopic features of ganglia and nerves evaluated in animal species commonly used in toxicity studies evaluating regulated products and chemicals. This atlas provides images of findings that may be encountered in ganglia and nerves of animal species commonly used in product discovery and development. Most atlas images are of tissues from control animals that were processed using routine methods (ie, immersion fixation in neutral-buffered 10% formalin, embedding in paraffin, sectioning at 5 μm , and staining with hematoxylin and eosin) since these preparations are traditionally applied to study materials produced during most animal toxicity studies. A few images are of tissues processed using special procedures (ie, immersion or perfusion fixation using methanol-free 4% formaldehyde, postfixation in glutaraldehyde and osmium, embedding in hard plastic resin, sectioning at 1 μm , and staining with toluidine blue), since these preparations promote better stabilization of lipids and thus optimal resolution of myelin sheaths. Together, this compilation provides a useful resource for discriminating among normal structures, procedure- and processing-related artifacts, incidental background changes, and treatment-induced findings that may be seen in PNS tissues of laboratory animals.

Keywords

autonomic nervous system, ganglion, nerve, axon, myelin, PNS

Introduction

Peripheral nervous system (PNS) toxicity is a common adverse effect in patients who have been exposed to certain chemicals (eg, pesticides and solvents) and drugs (eg, antineoplastic and antiretroviral agents).¹⁻⁵ Such clinical outcomes may occur without any indication suggesting the potential for PNS neurotoxicity during animal toxicity evaluations. This discrepancy likely reflects a combination of many factors: site-specific⁶ and strain-dependent⁷ variations in PNS responsiveness to neurotoxic agents, the repair capabilities of PNS tissues following insults, the paucity of functional screening tests capable of detecting peripheral neuropathies in most nonclinical safety assessment programs, limitations in pathology end points for PNS evaluation, differing responses elicited by various dosing regimens (acute, subacute, or chronic), the nature of the test article, and/or the subtle or intermittent nature of in-life clinical signs. In future, adjusted screening techniques (eg, expanded PNS sampling⁸) likely will improve our ability to translate

animal-derived PNS neurotoxicity data to predict possible responses in human cells, tissues, and systems.

The PNS is composed of 2 main divisions.⁹ The somatic (or sensorimotor) division is responsible for collecting sensory data and controlling effector organs that mediate voluntary functions. The autonomic division (or autonomic nervous system) supervises effector organs that undertake involuntary

¹ Pfizer Inc, Global Pathology, Groton, CT, USA

² AnaPath GmbH, Oberbuchsitzen, Switzerland

³ Tox Path Specialists, LLC (A StageBio Company), Frederick, MD, USA

⁴ Covance Laboratory, Inc, Madison, WI, USA

⁵ GEMpath, Inc, Longmont, CO, USA

[†] Posthumous

Corresponding Author:

Ingrid D. Pardo, Pfizer Inc, Global Pathology, 1 Eastern Point Rd, Groton, CT 06340, USA.

Email: ingrid.d.pardo@pfizer.com

homeostatic functions. The autonomic division is partitioned into several components including the parasympathetic, enteric, and sympathetic subdivisions. In general, parasympathetic elements facilitate resting functions, the enteric neural network innervates the digestive tract,¹⁰ and sympathetic elements control responses to stressful (ie, “fight or flight”) conditions. Neuropathologic evaluation of the PNS may involve any or all of these divisions depending on the nature of the test article and the constellation of in-life clinical signs.⁸

The somatic division of the PNS consists of sensory and motor components that are separated in space along the vertebral axis but typically are combined peripherally. Sensory elements of the somatic PNS include neurons in the dorsal root ganglia (DRGs) and their associated nerve fibers within dorsal spinal nerve roots and nerves as well as certain cranial nerves and their ganglia. Motor constituents of the somatic PNS consist of nerve fibers within the ventral spinal nerve roots and nerves, which arise from central nervous system (CNS) neurons in the ventral horn gray matter of the spinal cord, as well as some cranial nerves and their ganglia. The DRGs are bilaterally paired collections of sensory neurons, one set for each spinal cord segment, that are located between the lateral processes of adjacent vertebrae.⁸ The DRGs are connected to the spinal cord by dorsal spinal nerve roots; the DRG neurons are interspersed among fibers of the dorsal root. The DRGs are richly supplied with blood vessels¹¹ and are not protected by a neurovascular barrier (“blood–nerve barrier”) or dense connective tissue capsule.¹² For some body regions, nerve fibers from multiple DRGs coalesce into plexuses located near the central axis that subsequently supply nerve trunks to more peripheral sites (eg, the brachial plexus for the forelimb and the lumbosacral plexus for the hindlimb). The contributions to major spinal nerve trunks vary among species and across strains.^{8,13} The trigeminal (cranial nerve V) ganglia (also called the Gasserian or semilunar ganglia) are the main cranial nerve ganglia that are examined routinely for possible PNS neurotoxic effects. These bilaterally paired ganglia are collections of sensory neurons located at the base of the skull, typically bracketing the pituitary gland.¹⁴ Branches of the trigeminal nerve include both sensory and motor fibers.

The autonomic division of the PNS consists of the parasympathetic, enteric, and sympathetic ganglia and their associated preganglionic and postganglionic nerves. The reach of these autonomic subdivisions varies considerably within the body. The parasympathetic subdivision supplies tissues only of the head, viscera, and external genitalia; the enteric subdivision is limited to the digestive tract; and the sympathetic subdivision is distributed to nearly all tissues within the body. The ganglia for the parasympathetic and enteric subdivisions are located close to or within the organs that they innervate, so the preganglionic nerves are long. Traditionally, preganglionic fibers for these 2 subdivisions have been understood to pass from the CNS via cranial and sacral nerves,⁹ although recent research suggests that the sacral nerves may actually transmit sympathetic fibers.¹⁵ In contrast, the ganglia for the sympathetic

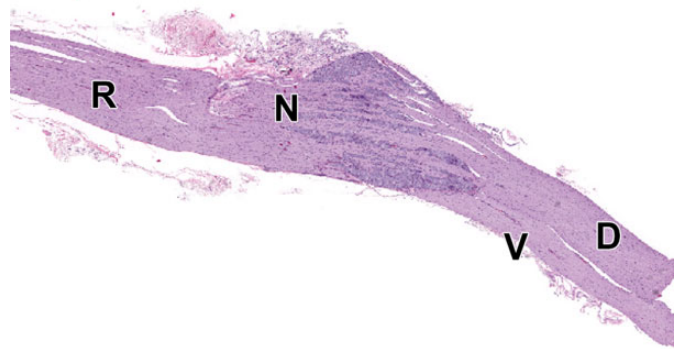


Figure 1. Dorsal root ganglion (DRG) and spinal roots at cervical spinal cord segment C₁. D = dorsal spinal nerve root composed of somatic and autonomic nerve fibers (ascending sensory information passing to CNS). N = neurons forming the DRG. R = spinal nerve containing both sensorimotor and autonomic nerve fibers. V = ventral spinal nerve root composed of motor and autonomic nerves (descending motor information arising from the CNS). Species: 12-week-old, male, Wistar rat. Processing: NBF immersion, paraffin, H&E. CNS indicates central nervous system; H&E, hematoxylin and eosin; NBF, neutral-buffered 10% formalin.

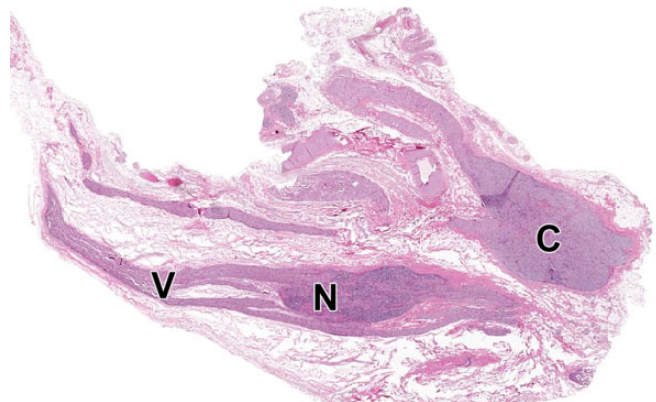


Figure 2. Caudal vagal and cranial cervical ganglia. N = caudal (“inferior” [in bipeds]) vagal (or “nodose”) ganglion, a parasympathetic sensory ganglion associated with the V = vagus nerve (cranial nerve X). C = cranial (or “superior” [in bipeds]) cervical ganglion, the most cranial sympathetic chain ganglion. Species: Adult, male, Beagle dog. Processing: NBF immersion, paraffin, H&E. H&E indicates hematoxylin and eosin; NBF, neutral-buffered 10% formalin.

subdivision are located near the central axis in proximity to the vertebral column and give rise to long postganglionic nerves that innervate viscera, vessels, and glands. The preganglionic fibers for the sympathetic subdivision emerge from the CNS via the thoracic and lumbar nerves (and possibly the sacral nerves¹⁵). Locations of major parasympathetic and sympathetic ganglia of potential interest for PNS neuropathology evaluation may be obtained from published or Internet-based anatomy resources.^{8,9,16–18} A simple means for sampling 2

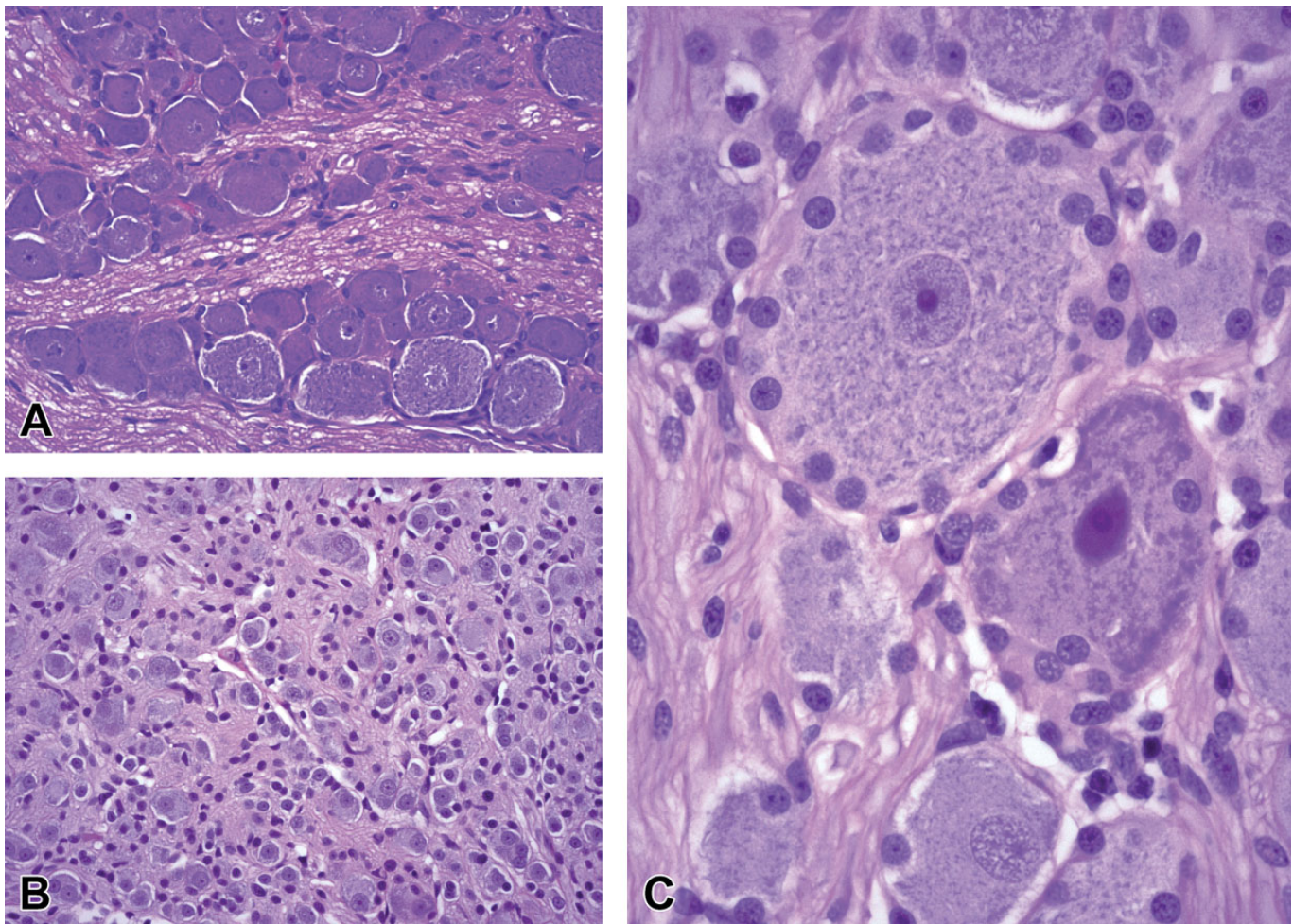


Figure 3. Comparison of neuron phenotypes in somatic (A and C) and autonomic (B) ganglia. A, Dorsal root ganglion (DRG) from level T₆ of the thoracic spinal cord demonstrating intermingled large-diameter (“type A”) and small-diameter (type B”) neurons; original objective = ×20. B, Parasympathetic ganglion from prostate gland demonstrating close packing of many small neurons and satellite cells; original objective = ×20. C, Large-diameter neurons encircled by small, round nuclei of satellite glia cells from a DRG at level L₄ of the lumbar spinal cord. Species: Juvenile, male cynomolgus monkey. Processing: NBF immersion, paraffin, H&E. H&E, hematoxylin and eosin; NBF, neutral-buffered 10% formalin.

specific autonomic ganglia in animals is to harvest the caudal vagal ganglion (a parasympathetic visceral afferent [sensory] element, designated the “inferior vagal” or “nodose” ganglion in bipeds) along with the cranial cervical ganglion (a sympathetic element, designated the “superior cervical” ganglion in bipeds). These 2 ganglia are located adjacent to each other just caudal (or ventral in bipeds) and lateral to the larynx.⁸

This atlas has been compiled to facilitate the detection of morphologic changes in PNS tissues during animal toxicity studies. More importantly, the images have been assembled to permit ready comparison of possible test article–related effects with other PNS features that might confound interpretation, including normal structures, incidental background changes, and procedure- and processing-related artifacts. Correct differentiation of these findings is necessary for successful PNS neuropathology evaluation.

Instructions for Using the Atlas

This atlas is divided into 4 sections. In order, sections cover (1) normal microanatomic structures, (2) procedure- and processing-related artifacts, (3) spontaneous background findings, and (4) key neurotoxic lesions. For each section, features in both ganglia and nerves are shown. Where warranted, both the somatic and the autonomic divisions of the PNS are covered.

The following conventions were employed in constructing the figure legends. Each image was given a short title (presented in bold text), which was followed by a detailed description enumerating key attributes of the image and the meanings of any annotated features. Legends continue by identifying the tissue (if not already stated) and species. The final portion of each legend defined the processing conditions, using the following abbreviations to communicate the principal elements:

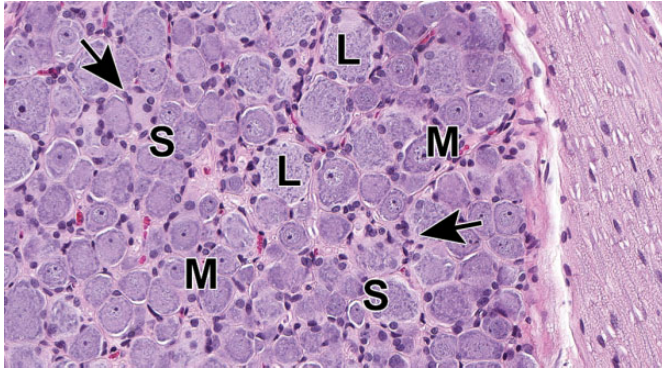


Figure 4. Dorsal root ganglion (DRG) from lumbar spinal cord segment L₄. The complement of neurons includes large-diameter (L), medium-sized (M), and small-diameter (S) cells, and satellite glia cells (arrows) are common. Accurate assignment of neuronal size is possible only when the nucleus can be observed within the cell body (which confirms that the cell has been sectioned through the center rather than tangentially). Species: Juvenile cynomolgus monkey. Processing: NBF immersion, paraffin, H&E. H&E indicates hematoxylin and eosin; NBF, neutral-buffered 10% formalin.

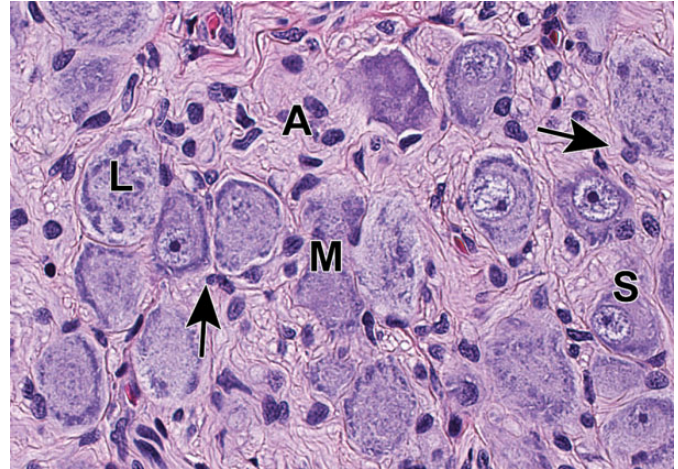


Figure 6. Cranial cervical ganglion, a sympathetic ganglion that contains a mixture of large-diameter (L), medium-sized (M), and small-diameter (S) neurons. This distinction is important since this ganglion commonly is sampled together with the caudal vagal (“nodose”) ganglion (Figure 5), a neighboring parasympathetic ganglion comprised of uniformly large-diameter neurons. Arrows depict satellite glia cells. A = Sympathetic nerve fibers. Species: Adult, male Beagle dog. Processing: NBF immersion, paraffin, H&E (original objective = $\times 40$). H&E indicates hematoxylin and eosin; NBF, neutral-buffered 10% formalin.

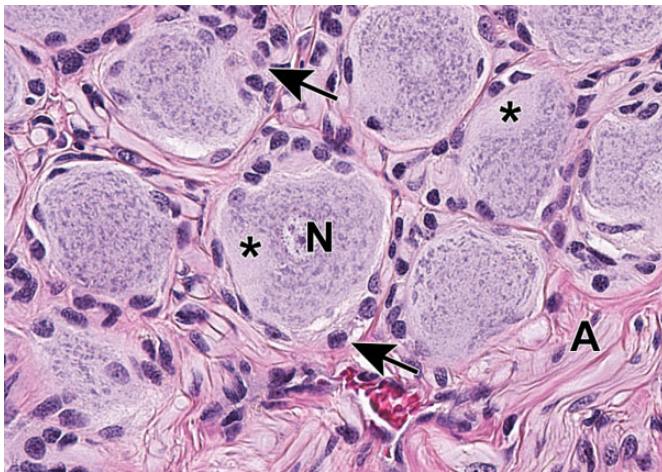


Figure 5. Caudal vagal (“nodose”) ganglion characterized by a uniform population of large-diameter sensory neurons (N) and numerous satellite glia cells (arrows). A = vagal nerve fibers. Asterisks = axon hillocks. Species: Adult, male Beagle dog. Processing: NBF immersion, paraffin, H&E (original objective = $\times 40$). H&E indicates hematoxylin and eosin; NBF, neutral-buffered 10% formalin.

- Fixation strategy
 - Immersion = immersion fixation after tissue removal at necropsy
 - Perfusion = whole-body perfusion fixation in situ followed by tissue removal and additional immersion fixation in fresh fixative
- Fixative type
 - NBF = neutral-buffered 10% formalin (containing methanol as a stabilizer)
 - MFF = methanol-free 4% formaldehyde (known colloquially as “4% paraformaldehyde”)

- Glut = glutaraldehyde (2.5% to 4%) perfusion fixation or immersion postfixation
- Osm = osmium tetroxide (1%) postfixation by immersion
- Embedding medium
 - Paraffin = paraffin embedding
 - Plastic = hard plastic resin embedding
- Staining
 - H&E = hematoxylin and eosin
 - LFB = Luxol fast blue
 - TB = toluidine blue

Knowledge of the exact processing conditions is essential when evaluating PNS sections, since myelin quality varies substantially depending on the fixation strategy, fixative type, and embedding medium.

Normal Microanatomic Structures of the PNS

This section contains images of normal PNS structures. Many of these structures may appear in standard PNS samples from general toxicity studies, while others are more likely to be observed only when additional PNS sampling has been performed as part of a detailed neurotoxicity study.⁸ Familiarity with these PNS characteristics is essential to avoid incorrectly interpreting such normal features as test article–related effects.

Ganglia in the PNS are collections of neurons and glia embedded in a web of intermingled nerve fibers, connective tissue, and capillaries (Figure 1). The glia in ganglia are termed “satellite” glia cells, and they serve the same basic functions as

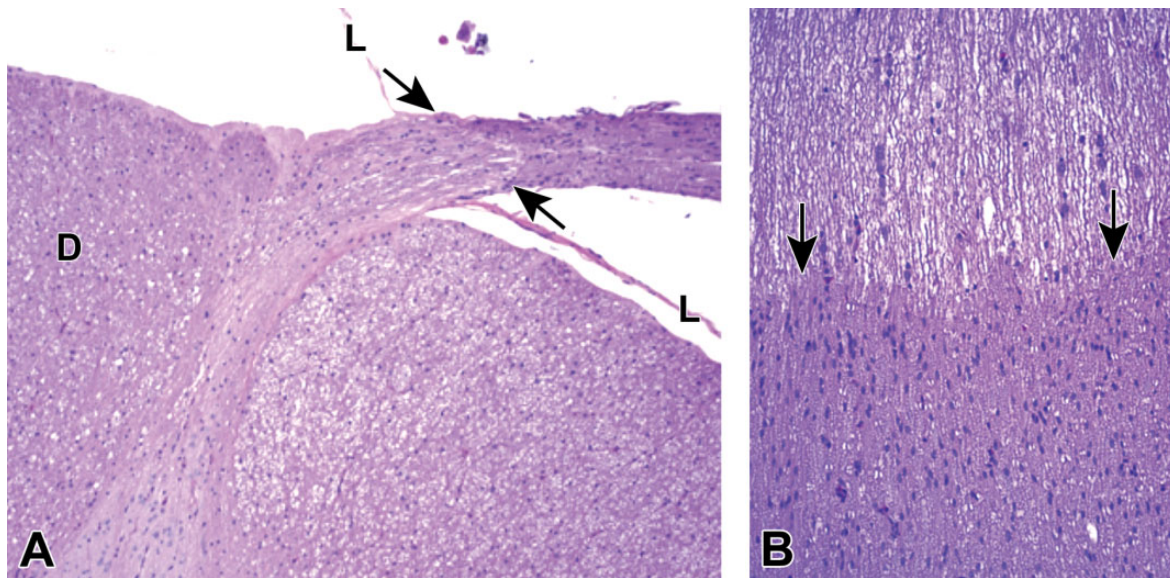


Figure 7. Origin of the dorsal spinal nerve root from the lumbar spinal cord. A, The transition from CNS origin (oligodendrocyte-generated) myelin to PNS origin (Schwann cell-derived) myelin is denoted by arrows. B, Pale-stained CNS myelin is characterized by rows of round oligodendrocyte nuclei, while the dark-stained PNS myelin contains large numbers of randomly dispersed, oval Schwann cell nuclei. D = dorsal funiculus of the spinal cord. L = leptomeninges. Species: Immature, male cynomolgus monkey. Processing: NBF immersion, paraffin, H&E. CNS, central nervous system; H&E, hematoxylin and eosin; NBF, neutral-buffered 10% formalin; PNS, peripheral nervous system.

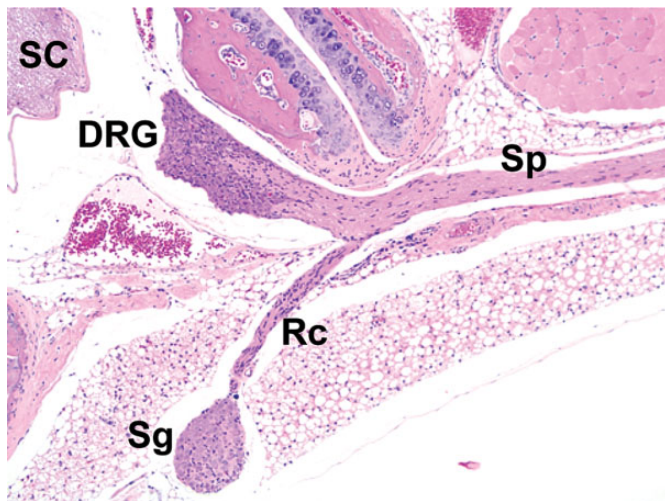


Figure 8. Distribution of somatic and autonomic branches of a spinal nerve. A thick spinal nerve trunk (Sp) courses peripherally from its dorsal root ganglion (DRG), giving off a narrow ramus communicans (Rc) that carries autonomic nerve fibers to a nearby sympathetic chain ganglion (Sg). SC = spinal cord. Species: Adult mouse (strain unspecified). Processing: NBF immersion, paraffin, H&E. Image adapted from Snyder et al²⁴ with permission from Academic Press. H&E indicates hematoxylin and eosin; NBF, neutral-buffered 10% formalin.

astrocytes within the CNS.^{19,20} Nerves are comprised of bundled nerve fibers, where each fiber represents an axon enveloped by its associated Schwann cell (glial) coating as either myelin (ie, laminated Schwann cell plasma membrane) or cell processes. Schwann cell functions in the PNS mirror those of oligodendrocytes in the CNS. Occasionally, other cell

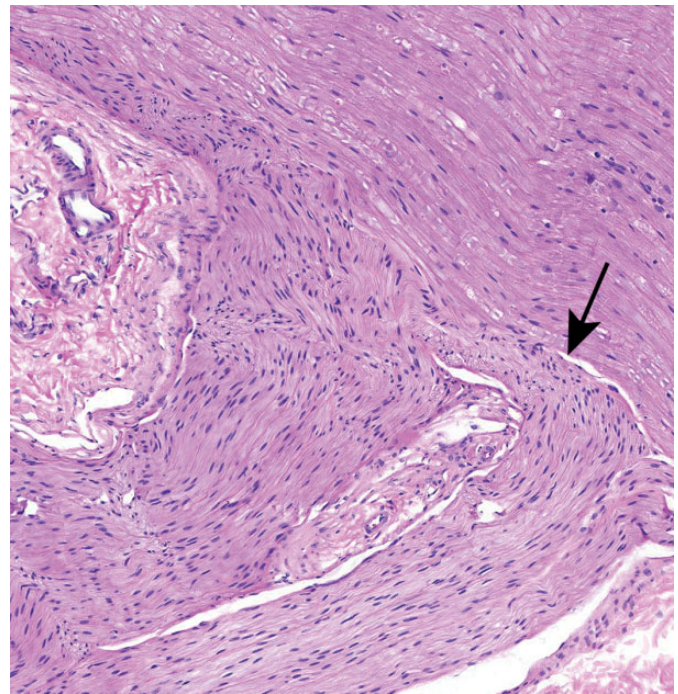


Figure 9. Branching of an autonomic nerve (arrow) from a sacral spinal nerve root. Autonomic nerves (characterized by small-diameter, unmyelinated nerve fibers) often can be found in association with somatic nerves (which contain both large-diameter, myelinated nerve fibers and small-diameter, thinly or unmyelinated fibers). An important consideration in PNS evaluation is to recognize that the variable morphology of normal autonomic branches (relative to the adjacent spinal nerves) should not be interpreted as evidence of nerve degeneration. Species: Rhesus monkey. Processing: NBF immersion, paraffin, H&E. H&E indicates hematoxylin and eosin; NBF, neutral-buffered 10% formalin; PNS, peripheral nervous system.

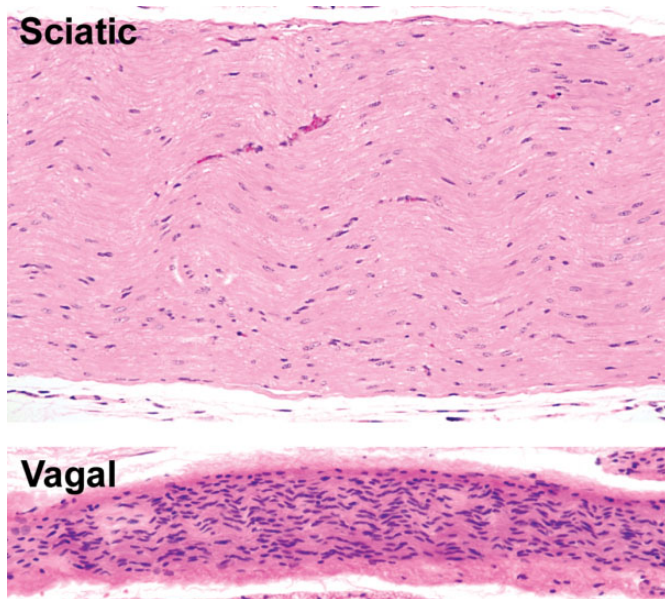


Figure 10. Comparison of morphological features in somatic and autonomic nerve trunks. The thickly myelinated sciatic nerve, a spinal-origin somatic nerve, is characterized by abundant eosinophilic myelin and relatively few Schwann cells. The vagal nerve (cranial nerve X), an autonomic trunk intermingling thinly myelinated and unmyelinated nerve fibers, is characterized by myriad Schwann cells and little eosinophilic myelin. Species: Adult mouse (strain unspecified). Processing: NBF immersion, paraffin, H&E. H&E indicates hematoxylin and eosin; NBF, neutral-buffered 10% formalin.

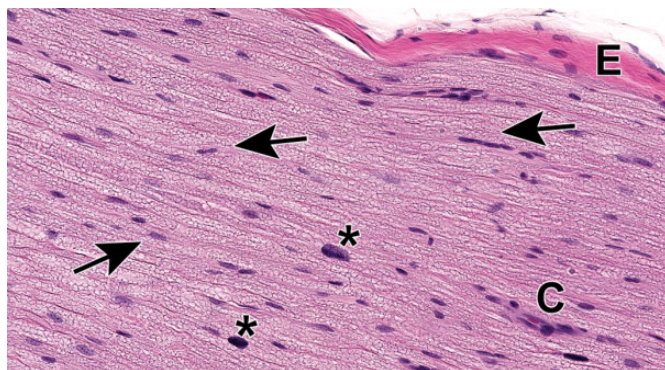


Figure 11. Sciatic nerve demonstrating the abundant eosinophilic myelin and scattered Schwann cell nuclei (arrows) that are the characteristic features of the most common PNS sample in animal toxicity studies. Asterisks = mast cells (which occur occasionally as a normal feature in rodent nerves). C = capillary. E: epineurium. Species: 12-week-old, male Wistar rat. Processing: MFF immersion, paraffin, H&E. H&E indicates hematoxylin and eosin; MFF, methanol-free 4% formaldehyde.

types—chiefly lymphocytes, macrophages, and mast cells—may also be observed within ganglia and nerves.

Ganglia of various PNS divisions may appear in proximity to one another (Figure 2). In such cases, microanatomic features of neurons as well as the pattern of neuron distribution may be utilized to discriminate the various classes of neurons.

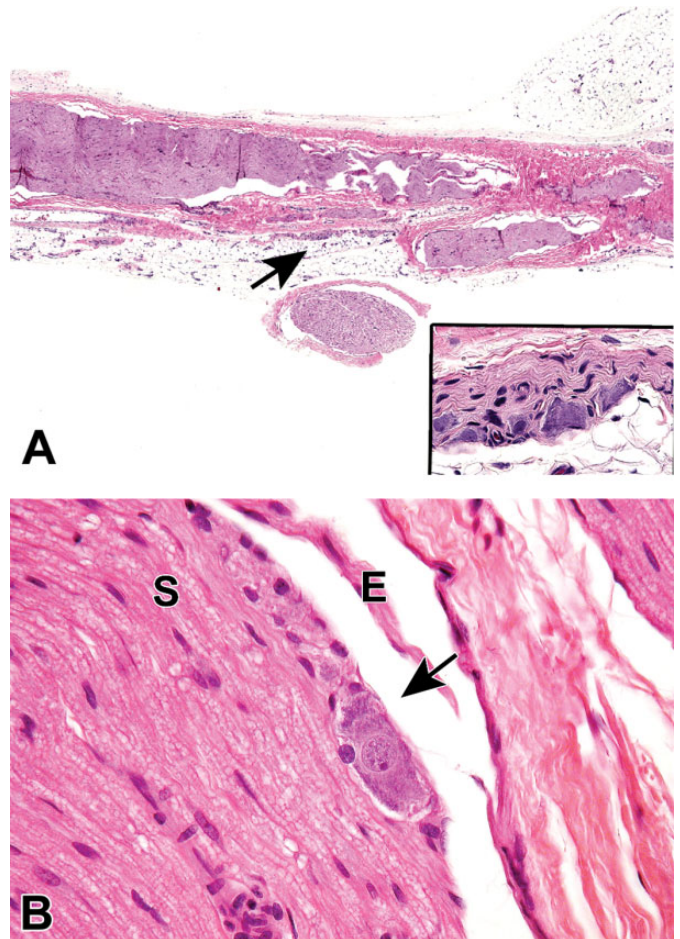


Figure 12. Autonomic neurons and unmyelinated nerve fibers (arrows and inset, panels A and B) adjacent to the epineurium (E) of the sciatic nerve (S). The autonomic nature of these foci is suggested by the high density of Schwann cell nuclei within these regions. Care must be taken in making this interpretation as somatic nerves also contain small-diameter, thinly, or unmyelinated nerve fibers. Species: 12-week-old, male Wistar rat. Processing: NBF immersion, paraffin, H&E. H&E indicates hematoxylin and eosin; NBF, neutral-buffered 10% formalin.

In DRGs (Figures 3A and C and 4), the main neuronal phenotypes based on structure are large-diameter (“type A”) and small-diameter (“type B”) cells.²¹ The large-diameter neurons transmit non-nociceptive signals from the periphery to laminae III-V of the spinal cord dorsal horn via large-caliber, thickly myelinated A β fibers, while the small-diameter (“type B”) neurons convey mechanoreceptive, nociceptive, and thermal signals to lamina I-II of the spinal cord dorsal horn via small-caliber unmyelinated C-fibers or thinly myelinated A β fibers. While outside the scope of this article, DRG neurons may be further classified based on other morphologic and biochemical features.^{22,23} In autonomic ganglia, neurons vary in size from uniformly small (Figure 3B) to uniformly large (Figure 5) to a mixture of sizes (Figure 6) depending on the ganglion location and cellular function.

Nerves arise from the brain stem (cranial nerves) or spinal cord (Figure 7) and course distally, branching at various points

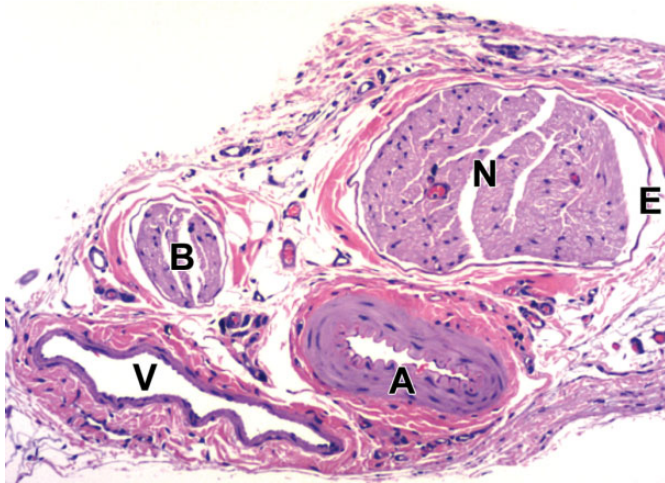


Figure 13. Spinal nerves (N) and their branches (B) are distributed in association with arteries (A) and veins (V). E = epineurium. Sural nerve. Species: Adult, female Sprague-Dawley rat. Processing: NBF immersion, paraffin, H&E. H&E indicates hematoxylin and eosin; NBF, neutral-buffered 10% formalin.

(Figures 8 and 9), so that nerve fibers with distinct functions can reach their intended target tissues by a relatively direct route. Nerve form depends on function. In general, sensorimotor trunks contain both large-diameter nerve fibers with thick myelin sheaths and relatively dispersed Schwann cell nuclei to allow high-velocity impulse conduction as well as small-diameter nerve fibers with little or no myelin that permit slow-velocity transmission (Figures 10 and 11), while autonomic nerves have small-diameter, thinly myelinated or unmyelinated nerve fibers with more densely clustered Schwann cell nuclei that permit slower transit of homeostatic information (Figures 10 and 12). Somatic and autonomic nerves may be located in proximity to each other, and sometimes autonomic neurons may occur within these nerves as isolated cells or small aggregates located far from ganglia (Figure 12). Nerves tend to course parallel to adjacent blood vessels (Figure 13), so that nearby arteries serve not only as landmarks to locate small distal nerve branches but also as a stiff internal scaffold to permit nerve harvesting with less damage to the fragile nerve tissue. When viewed in cross section, spinal nerves may be seen to consist of numerous large-diameter fibers with thick nerve sheaths interspersed with aggregates of small-diameter, thinly myelinated, or unmyelinated nerve fibers; such details are best appreciated in hard plastic resin-embedded sections stained with toluidine blue (Figure 14). Each myelinated nerve fiber consists of a continuous series of internodes (ie, the distance between 2 nodes of Ranvier that is spanned by one Schwann cell), where each internode is formed by an individual axon enveloped by tightly wrapped concentric lamellae of plasma membrane arising from a single myelinating Schwann cell (Figure 15A). The internodal length generally is proportional to the axon diameter and in health remains fairly constant for a given nerve fiber, although it varies depending on the nerve location even for axons of similar

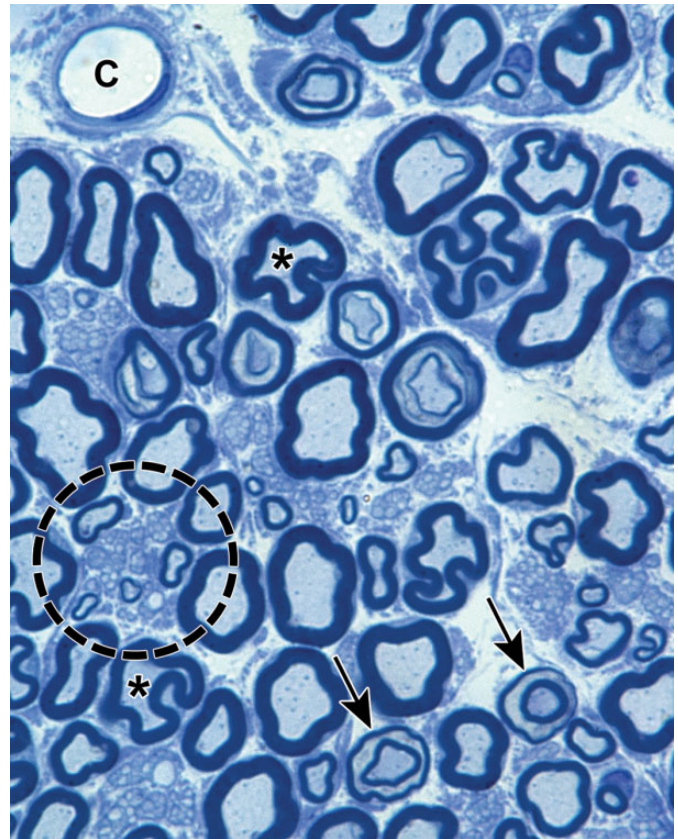


Figure 14. Distribution of nerve fibers within a spinal nerve. Numerous large-diameter myelinated fibers (evident as pale-stained, large axons encircled by thick rings of dark-stained myelin) are intermingled with scattered clusters (dashed circle) of thinly myelinated and unmyelinated fibers (seen as pale-stained, small axons surrounded by thin myelin layers or no myelin). Myelinated fibers (typically 2-20 mm in diameter) serve immediate somatic functions, while unmyelinated or thinly myelinated fibers (usually 0.2-3.0 mm in diameter) fulfill slower functions (eg, monitoring pain and temperature and transmitting efferent autonomic signals). Unusual features of nerve fibers visible in hard plastic sections include myelin (Schmidt-Lanterman) incisures (arrows), which are lakes of residual cytoplasm separating myelin layers, and axon fluting (asterisks), which appears as infolding of myelin sheaths in proximity to nodes of Ranvier. C = capillary (with one visible endothelial cell nucleus). Sciatic nerve. Species: Adult rat (strain unspecified). Processing: Glut (4%) perfusion, Osm immersion, plastic, 1- μ m-thick section, TB. Glut = glutaraldehyde, Osm = osmium tetroxide, TB = toluidine blue. Image courtesy of Dr William Valentine.

diameter. In contrast, unmyelinated fibers are apparent as clusters of axons encompassed by cytoplasmic processes of a single non-myelinating Schwann cell (Figure 15B). For both myelinated and unmyelinated nerve fibers, each Schwann cell and the axon(s) it supports are surrounded by a basement membrane (Figure 15). Special stains are commonly used in PNS neuropathology evaluation to highlight axons and/or myelin, thereby affording a better view of their structural integrity (Figure 16).

Special PNS tissues may be observed regularly in some non-neural tissues that are sampled routinely during animal toxicity studies, and they should be recognized as normal constituents of the PNS and not lesions. For example, lamellar (Pacinian)

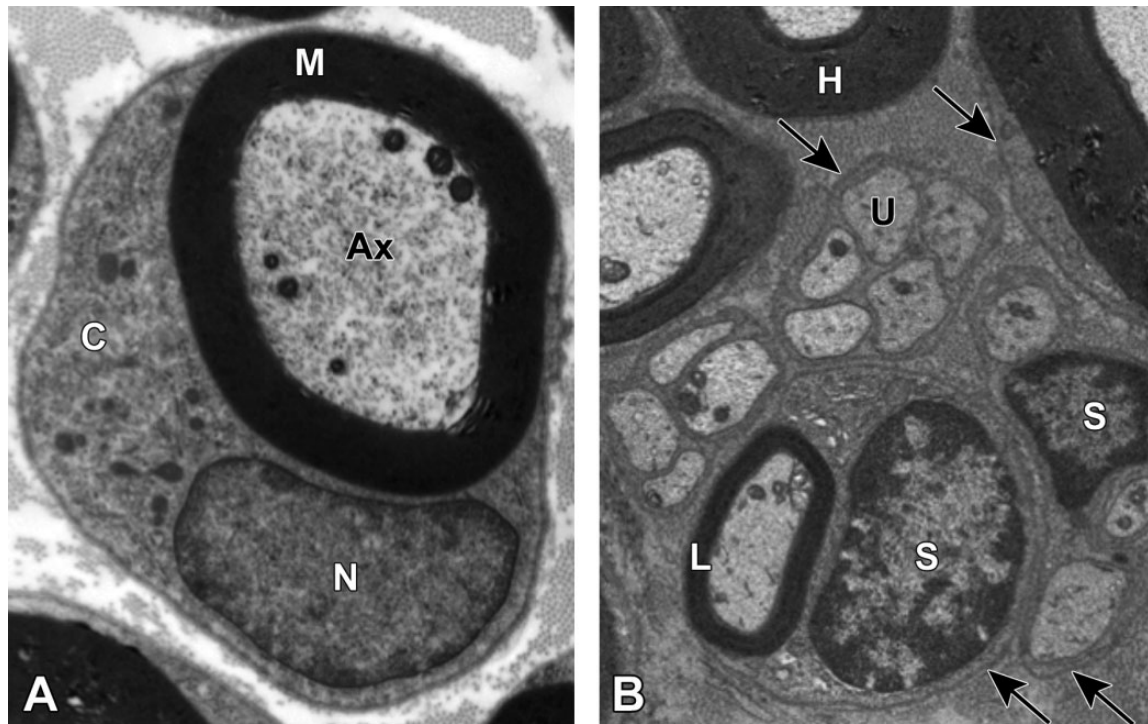


Figure 15. Comparison of myelinated and unmyelinated nerve fibers. A, Transmission electron micrograph demonstrating a large-caliber axon (Ax) with 6 mitochondria enveloped by a thick myelin sheath (M). The image is taken at the mid-internode (ie, halfway between two nodes of Ranvier) as indicated by the nucleus (N) and abundant cytoplasm (C) of the adjacent myelinating Schwann cell. Image courtesy of Dr William Valentine. B, Multiple nerve fibers are evident, including highly (H) and lightly (L) myelinated variants and clusters of unmyelinated (U) axons. A single Schwann cell (S) is responsible for producing the myelin sheath of the lightly myelinated fiber, while another Schwann cell has enveloped multiple unmyelinated fibers. Arrows denote the basement membrane surrounding the Schwann cell and its axon(s). Sciatic nerve. Species: Adult rat (strain unspecified). Processing (both panels): Glut (4%) perfusion, Osm immersion, plastic, 600-nm-thick section, uranyl acetate and lead citrate. Glut = glutaraldehyde, Osm = osmium tetroxide.

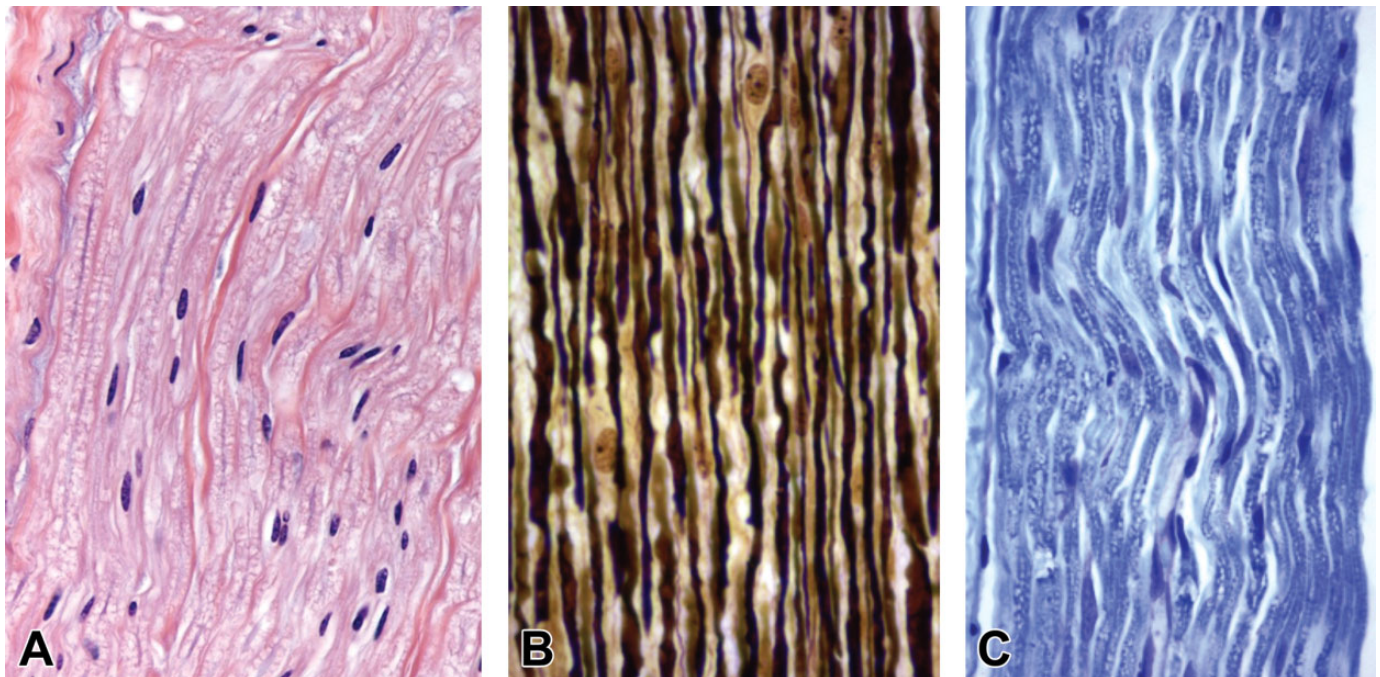


Figure 16. Comparison of common neurohistological staining procedures used for evaluating paraffin-embedded PNS sections in animal toxicity studies. A, Hematoxylin and eosin (H&E), the standard stain for screening, yields nerve fibers with abundant eosinophilic myelin and scattered, oval, basophilic Schwann cell nuclei. B, Bielschowsky's silver produces black axons and pale yellow myelin and Schwann cell nuclei. Intact axons appear as continuous, variably scalloped, linear profiles. C, Luxol fast blue (LFB) results in blue myelin, while axons are indistinct. Note: Tissue resolution in paraffin-embedded sections, even when viewed with special neurohistological stains, generally is lower relative to features visible in hard plastic resin-embedded sections stained with toluidine blue (compare to Figure 14). Species: Adult rat (strain unspecified). Processing: NBF immersion, paraffin, H&E. H&E indicates hematoxylin and eosin; NBF, neutral-buffered 10% formalin; PNS, peripheral nervous system.

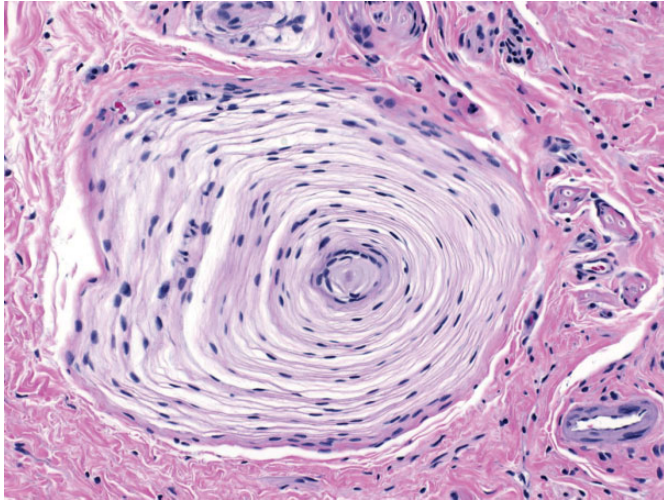


Figure 17. Lamellar (or Pacinian) corpuscles are multipurpose sensory receptors consisting of concentric lamellae surrounding a single central nerve fiber. Glabrous skin. Species: Juvenile, female cynomolgus monkey. Processing: NBF immersion, paraffin, H&E. H&E indicates hematoxylin and eosin; NBF, neutral-buffered 10% formalin.

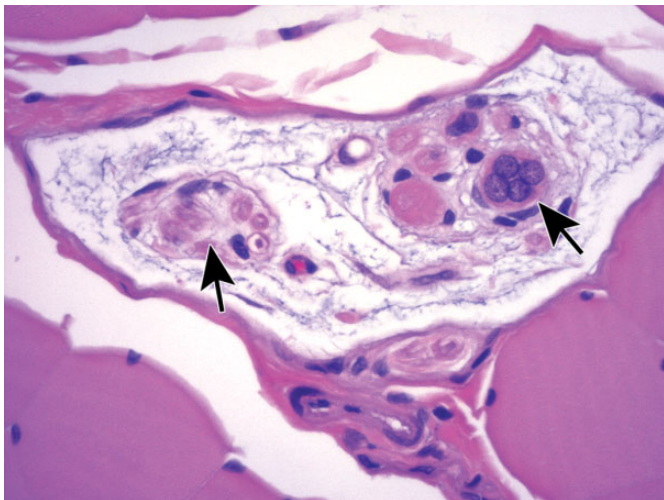


Figure 18. Muscle spindles are stretch receptors in skeletal muscle. These complex organs (arrows) are composed of small intrafusal muscle fibers entwined by sensory nerve endings, all supported by a fibrillar basophilic matrix and enclosed in a surrounding capsule. Gastrocnemius muscle (lateral head). Species: Adult mouse (strain unspecified). Processing: NBF immersion, paraffin, H&E. H&E indicates hematoxylin and eosin; NBF, neutral-buffered 10% formalin.

corpuscles are sensory receptors that detect pressure, tension, and vibration (Figure 17). These structures consist of multiple concentric lamellae surrounding a single central nerve fiber.²⁵ They may be observed in many tissues including joint capsules, ligaments, mesentery, and skin. Muscle spindles may be seen between myofibers of skeletal muscles (Figure 18). These organs are stretch receptors that monitor the length of the muscle belly, and they contribute to fine motor control by activating motor neurons responsible for the stretch reflex.²⁶ Other

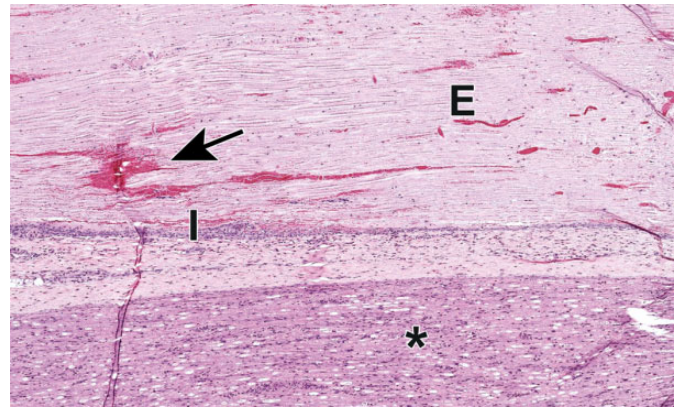


Figure 19. Procedural artifact due to acute ante mortem trauma of the sciatic nerve caused by a nearby deep intramuscular injection. Edema (E), hemorrhage (arrow), inflammation (I), and nerve fiber degeneration (asterisk) may be observed. Common injectables inciting this reaction include adjuvants (eg, in vaccines) and chemical restraint agents (eg, ketamine). Species: Juvenile cynomolgus monkey. Processing: NBF immersion, paraffin, H&E. H&E indicates hematoxylin and eosin; NBF, neutral-buffered 10% formalin.

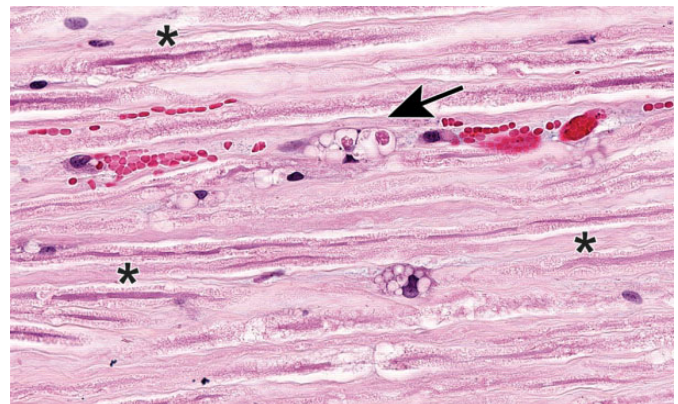


Figure 20. Edema (asterisk) and nerve fiber degeneration (arrow) as a procedural artifact due to acute ante mortem trauma of the sciatic nerve caused by a nearby deep intramuscular injection. Species: Juvenile cynomolgus monkey. Processing: NBF immersion, paraffin, H&E. H&E indicates hematoxylin and eosin; NBF, neutral-buffered 10% formalin.

receptor types have been defined (eg, bulbous [Ruffini] and tactile [Meissner's] corpuscles, free nerve endings, hair disks [Haarscheibe]),^{27–31} but these typically are not apparent in routinely harvested and prepared tissues from animal toxicity studies. These special PNS receptors can be damaged by some PNS neurotoxicants.^{32,33}

Procedural and Processing Artifacts

The structures of PNS tissues are exquisitely sensitive to disruption from both manipulative procedures (eg, trauma from ante mortem injections or post mortem sampling) and variations in processing conditions. Artifacts changes in PNS tissues can arise at many stages during in-life treatment, sample

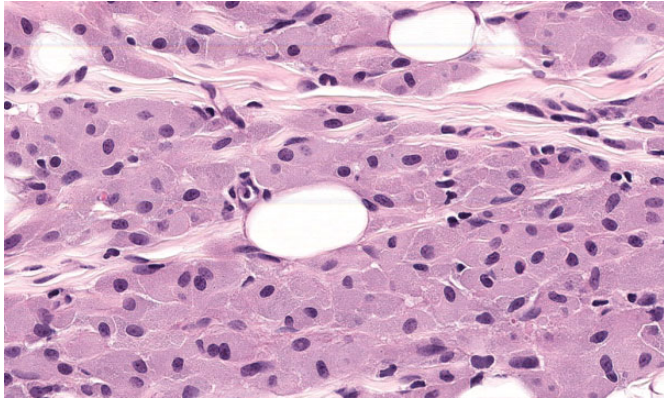


Figure 21. Accumulation of adjuvant-laden macrophages as a procedural artifact adjacent to the sciatic nerve due to a nearby deep intramuscular injection to administer a vaccine containing aluminum hydroxide. Species: Juvenile cynomolgus monkey. Processing: NBF immersion, paraffin, H&E. H&E indicates hematoxylin and eosin; NBF, neutral-buffered 10% formalin.

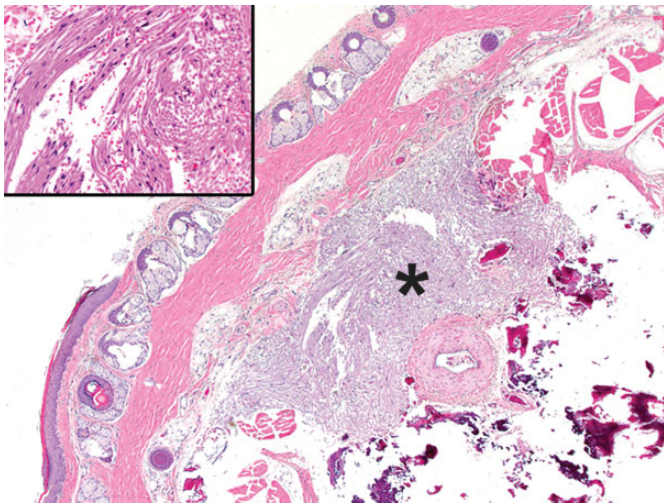


Figure 22. Posttraumatic neuroma (asterisk) as a procedural artifact in the tail, characterized by many disorganized bundles of nerve fibers. This finding, a consequence of failed nerve regeneration, may occur in the stump of an amputated extremity or in proximity to an intravenous injection that damages the adjacent soft tissues. Species: Adult Wistar rat. Processing: NBF immersion, paraffin, H&E. H&E indicates hematoxylin and eosin; NBF, neutral-buffered 10% formalin.

harvesting, and tissue processing. Artifacts associated with procedural- or processing-related damage often are misinterpreted as test article-induced effects. This dilemma can be prevented to a large extent by choosing appropriate PNS sampling and processing strategies when planning and performing animal toxicity studies.^{8,34-36} With experience, these artifacts can be distinguished reliably from spontaneous background findings and genuine test article-induced lesions.

Ante mortem trauma to PNS tissues falls into 2 categories. The first results from damage to PNS tissues, usually nerves, located adjacent to sites subjected to invasive procedures. For

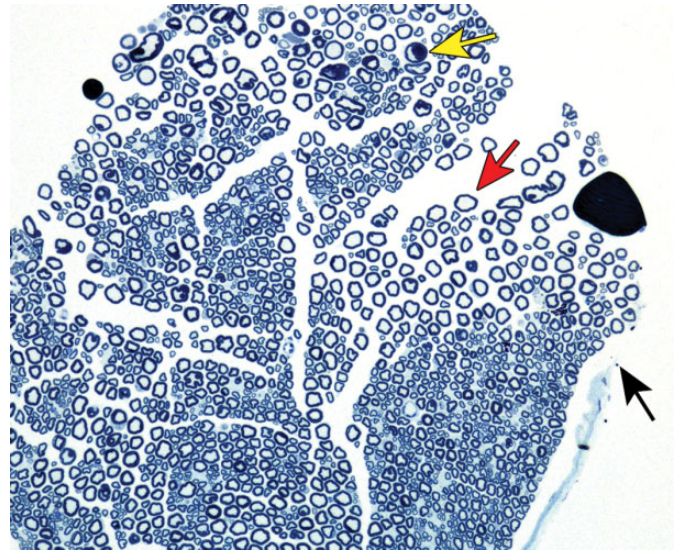


Figure 23. Procedural artifact due to aggressive handling of an inadequately fixed nerve at necropsy. The epineurium is no longer continuous (black arrow), the exposed myelinated nerve fibers are separating (red arrow), and some myelin sheaths are swollen (yellow arrow). Species: Mouse (strain unspecified). Processing: MFF/Glut perfusion, Osm postfixation, plastic, TB. MFF indicates methanol-free 4% formaldehyde, Glut = glutaraldehyde, Osm = osmium tetroxide, TB = toluidine blue.

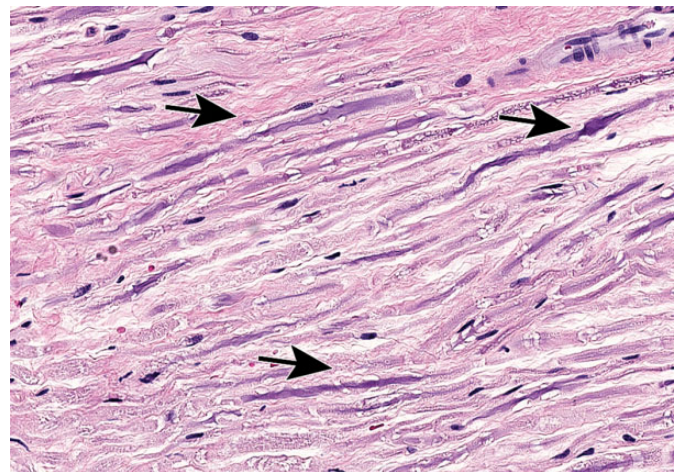


Figure 24. Procedural artifact due to excessive handling of an inadequately fixed nerve at necropsy. Nerve fibers are distorted, fragmented, and/or beaded (arrows) as a consequence of tissue crushing or stretching; these changes may be mistaken for nerve fiber degeneration and/or axonal dystrophy by inexperienced practitioners. Trigeminal nerve (cranial nerve V) root. Species: Adult Beagle dog. Processing: NBF immersion, paraffin, H&E. H&E indicates hematoxylin and eosin; NBF, neutral-buffered 10% formalin.

example, injection of irritating chemicals into tissues near nerves³⁷ (Figures 19 and 20) or traumatic blood collection from vascular plexuses adjacent to nerves³⁸ may induce nerve fiber degeneration as well as localized edema, hemorrhage, and/or inflammation. Over time, acute changes are repaired by an influx of macrophages into the areas of nerve

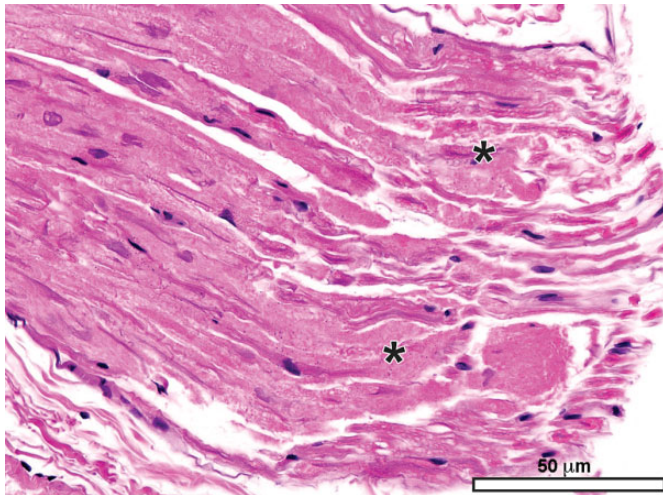


Figure 25. Procedural artifact due to excessive handling of an inadequately fixed nerve at necropsy. The cytoarchitecture of many nerve fibers is indistinct (asterisks). Sciatic nerve. Species: 12-week-old Crl: Wistar rat. Processing: NBF immersion, paraffin, H&E. H&E indicates hematoxylin and eosin; NBF, neutral-buffered 10% formalin.

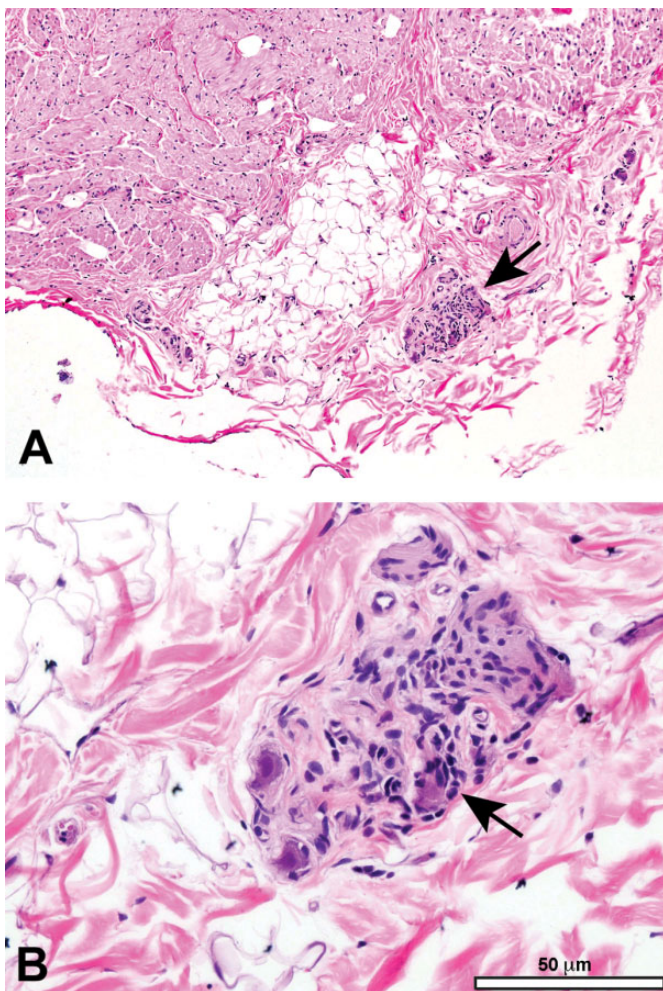


Figure 26. Procedural artifact due to excessive compression of an inadequately fixed cardiac parasympathetic ganglion at necropsy. A and B, The neurons and nerve fibers are shrunken and twisted (arrow); the distorted neurons may be mistaken for infiltrating mononuclear leukocytes by inexperienced practitioners. Species: 9-month-old Beagle dog. Processing: NBF immersion, paraffin, H&E. H&E indicates hematoxylin and eosin; NBF, neutral-buffered 10% formalin.

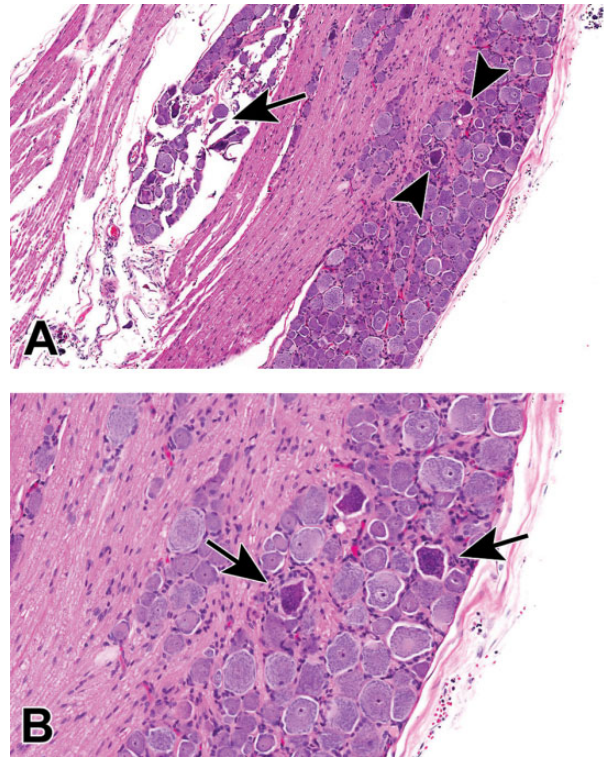


Figure 27. Procedural artifacts due to excessive handling of an inadequately fixed dorsal root ganglion at necropsy. A, Tissue separation (arrow) is evident where some neurons have pulled away from the remainder of the ganglion, while “dark neurons” (arrowheads) are scattered throughout the ganglion. B, Dark neurons (arrowheads) are angular, shrunken, and more basophilic than adjacent normal-appearing cells. Species: Adult Wistar rat. Processing: NBF immersion, paraffin, H&E. H&E indicates hematoxylin and eosin; NBF, neutral-buffered 10% formalin.

damage (Figure 21). Macrophage infiltrates are especially common at sites of adjuvant administration.³⁹ The second category of PNS change resulting from a traumatic in-life procedure is the formation of traumatic neuromas (Figure 22). These non-neoplastic masses consist of disorganized masses of nerve fibers. Neuromas usually form at sites where an appendage (eg, ear or tail) has been amputated, but on occasion they may develop near intravenous injection sites on the tail. In general, these findings can be linked to one or more specific instances of ante mortem trauma. However, to ensure that no difficulty in interpretation arises when evaluating PNS tissues, best practice for PNS sampling is to collect specimens of bilaterally symmetrical structures from both sides and to harvest nerve branches located at a distance from possible traumatic events.

Several issues arising at necropsy may induce artifacts in PNS tissues. For instance, aggressive handling of unfixed nerve tissue may rupture the epineurium (ie, dense connective tissue capsule that surrounds a nerve) and lead to separation of nerve fibers (Figure 23). In like manner, crushing or excessive stretching of unfixed PNS tissues at necropsy leads to distortion, expansion, and/or fragmentation of nerve fibers (Figures 24–26) that resemble nerve fiber degeneration or axonal dystrophy. Inadequate fixation of PNS tissues prior to processing frequently leads to one of the several artifacts. The first, observed in ganglia, is the genesis of “dark neurons” characterized by shrunken, angular profiles and dark basophilic

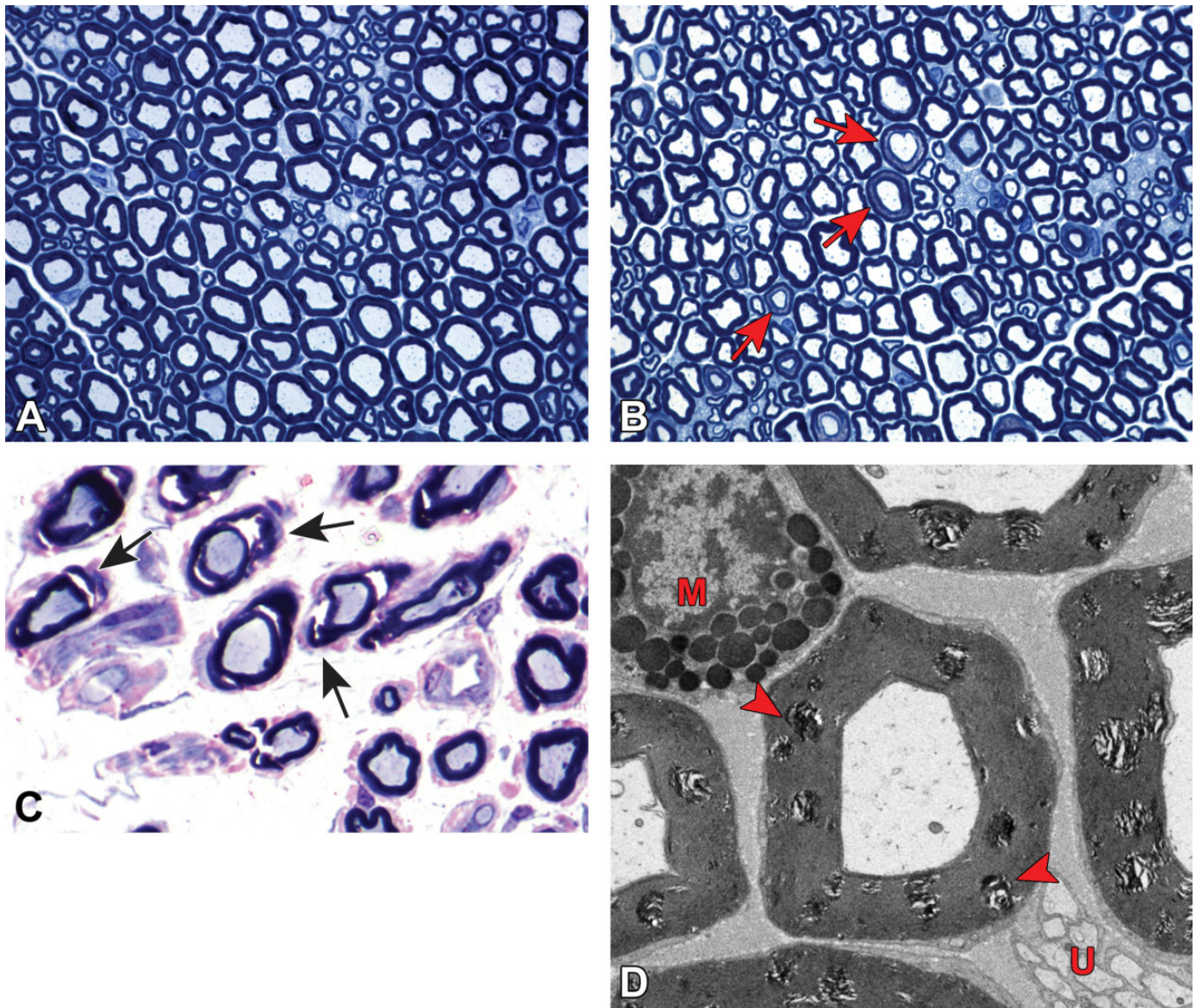


Figure 28. Myelin splitting as a procedural artifact due to inadequate fixation. A, Normal sciatic nerve is characterized by large-diameter, pale-stained axons of similar caliber with thick, intact, dark-stained myelin sheaths. B, Myelin (Schmidt-Lanterman) incisures (red arrows) appear as relatively uniform, narrow bands of pale-stained residual cytoplasm separating inner and outer rims of dark-stained myelin (see also Figure 14). C, Myelin splitting (arrows) is evident as widespread discontinuity of myelin (indicated by variably sized, pale-stained [fluid-filled] regions bracketed by dark-stained layers of intact myelin). D, In electron micrographs, myelin splitting from inadequate fixation presents as multifocal areas of irregular, pale-stained stippling within myelin sheaths (red arrowheads). M = mast cell. U = unmyelinated nerve fibers. Species: (A and B) = Adult mouse (strain unspecified); (C) = white Leghorn chicken; (D) = Adult Sprague-Dawley rat. Processing: (A and B) = MFF/Glut immersion, Osm postfixation, plastic, TB alone; (C) = Glut immersion, Osm postfixation, plastic, TB with safranin counterstain; (D) = MFF/Glut perfusion, Osm postfixation, plastic, uranyl acetate and lead citrate. MFF indicates methanol-free 4% formaldehyde, Glut = glutaraldehyde, Osm = osmium tetroxide, TB = toluidine blue.

coloration of the nucleus and cytoplasm (Figure 27).⁴⁰⁻⁴² This change typically is thought to arise from pressure applied to unfixed or underfixed ischemic neurons,⁴³ and its severity varies with neuron age⁴⁴ and the fixation procedure.^{45,46} In some instances, “dark neurons” have been demonstrated under strictly controlled experimental conditions to be induced by metabolic alterations,⁴⁷⁻⁵⁰ seizures,^{51,52} or xenobiotic treatments⁵³; to the authors’ knowledge, experimentally induced dark neurons reflect observations of changes

in CNS neurons and not those in PNS ganglia. The second, seen most often in large-diameter myelinated nerves, is myelin splitting due to insufficient cross-linking of macromolecules, which results in spreading of the myelin lamellae during dehydration (Figure 28). Finally, inadequate perfusion fixation that fails to flush all blood constituents from small vessels may permit establishment of protein clots in capillaries (Figure 29), which may be misinterpreted as axonal dystrophy. These artifacts may be reduced significantly by

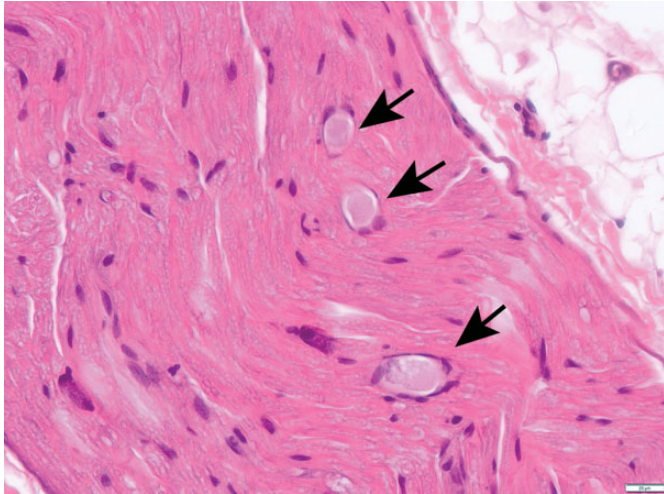


Figure 29. Procedural artifact due to inadequate vascular perfusion at necropsy. Distended blood vessels (identifiable by the curved endothelial cell nuclei) are filled with acellular, pale-stained eosinophilic material consistent with intravascular protein clots (arrows); these structures may be misinterpreted as axonal dystrophy by inexperienced practitioners. Sciatic nerve. Species: Adult male RccHan:Wistar rat. Processing: NBF immersion, paraffin, H&E. H&E indicates hematoxylin and eosin; NBF, neutral-buffered 10% formalin.

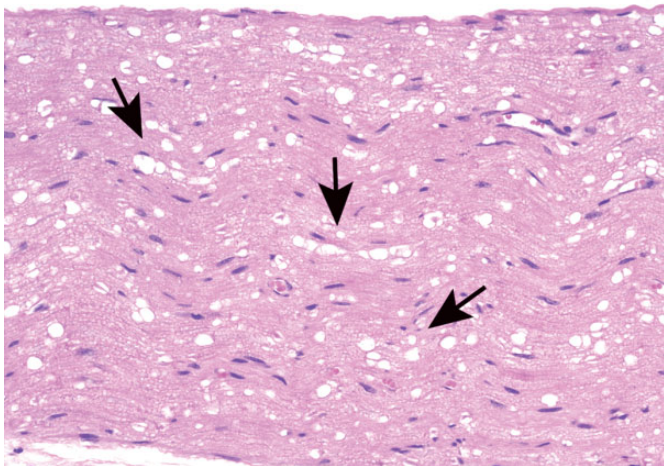


Figure 30. Vacuolation of myelin sheaths as a processing artifact. This change (arrows) may occur following prolonged immersion in an alcohol-containing fixative or alcohol-containing station on an automated tissue processor. The extent of vacuolation rises with increases in the concentration and/or length of time in alcohol. Sciatic nerve. Species: Adult mouse (strain unspecified). Processing: NBF immersion, paraffin, H&E. H&E indicates hematoxylin and eosin; NBF, neutral-buffered 10% formalin.

taking appropriate care in planning, obtaining, and preserving PNS tissues at necropsy.

Processing conditions play a substantial role in maintaining the structural integrity of PNS tissues. Extended exposure to alcohol-containing fixatives or dehydrating solutions (eg, by leaving PNS tissues on the tissue processor over the weekend)

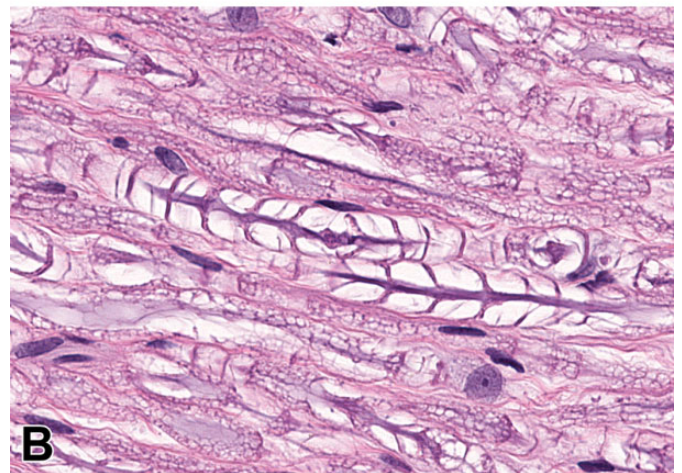
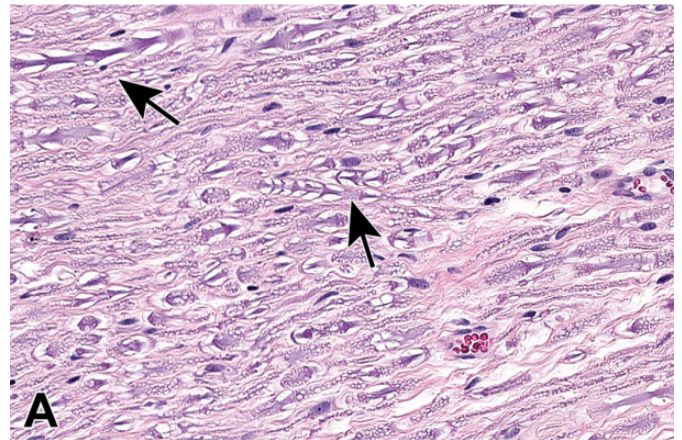


Figure 31. Neurokeratin formation as a processing artifact (arrow). A fine mesh of insoluble keratin-like protein is seen in myelin sheaths of routinely processed, paraffin-embedded tissue. The finding typically is explained as a consequence of lipid extraction using organic solvents (eg, alcohol and toluene) in tissue processing, although deposition of impurities in commercial NBF preparations has also been invoked. This material appears as black-stained foreign bodies in transmission electron micrographs. Note: The wide, clear, colorless spaces separated by thin, angled, basophilic branches evident in the 2 central nerve fibers represent myelin (Schmidt-Lanterman) incisures that have been artifactually expanded by accumulated fluid. Trigeminal nerve. Species: Adult, male Beagle dog. Processing: NBF immersion, paraffin, H&E. H&E indicates hematoxylin and eosin; NBF, neutral-buffered 10% formalin.

promotes vacuolation of myelin (Figure 30) or formation of insoluble neurokeratin (Figure 31) in nerves. Artifacts vacuoles in sensory neuron cytoplasm are also a common feature in DRGs (Figures 32 and 33) and, less often, autonomic ganglia (Figure 34). The mechanism responsible for these artifactual vacuoles has not been defined, but hypotheses include imbibition of fluid into cytoplasmic organelles, dissolution of accumulated protein depots, and/or traction-related forces encountered during tissue collection that cause separation among adjacent cells. Treatment-related vacuolation of DRG neurons has been reported and is attributed to hydropic degeneration (ie, intracellular fluid accumulation).⁵⁴⁻⁵⁶ Care must be exercised when interpreting neuronal vacuolation as an artifact

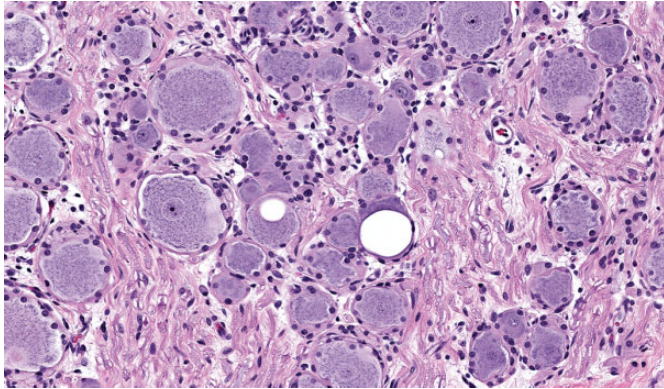


Figure 32. Intraneuronal vacuoles in dorsal root ganglion neurons as a processing artifact. Well-demarcated, variably sized, usually round, clear cytoplasmic vacuoles occur in large sensory neurons. The mechanism responsible for these artifactual vacuoles has not been determined. Note: Neuronal vacuoles associated with xenobiotic exposure, which may exhibit a similar appearance, result from hydropic degeneration. Species: Juvenile cynomolgus monkey. Processing: NBF immersion, paraffin, H&E. H&E indicates hematoxylin and eosin; NBF, neutral-buffered 10% formalin.

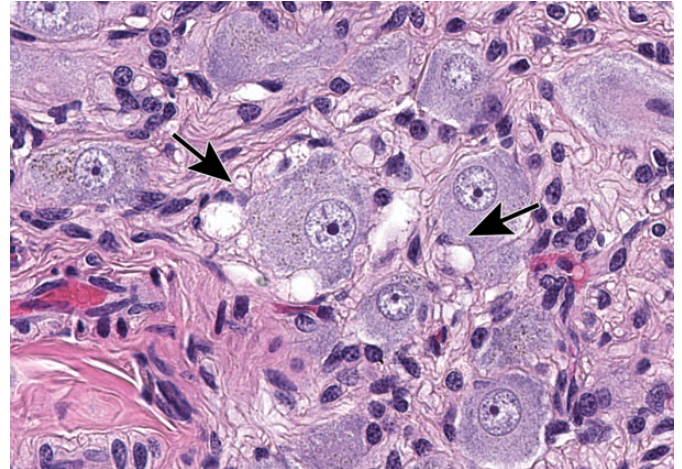


Figure 34. Intraneuronal vacuoles in autonomic (superior cervical) ganglion neurons as a processing artifact. Many well-demarcated, variably sized, irregularly oval, clear cytoplasmic vacuoles occur in occasional neurons (arrows). This finding may arise due to excessive traction applied during tissue collection and processing. Species: Juvenile cynomolgus monkey. Processing: NBF immersion, paraffin, H&E. H&E indicates hematoxylin and eosin; NBF, neutral-buffered 10% formalin.

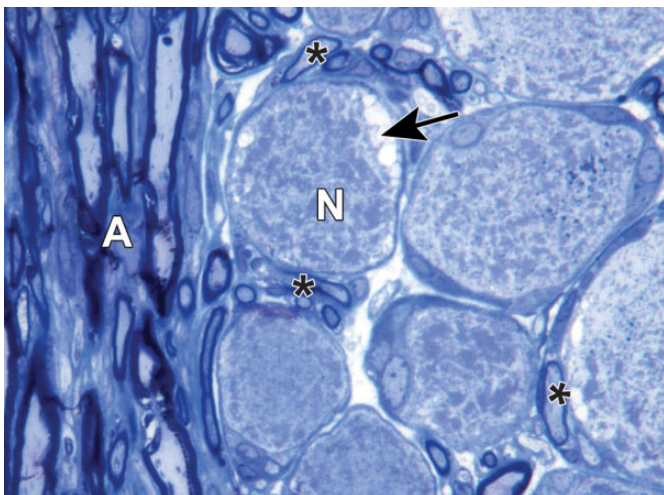


Figure 33. Intraneuronal vacuoles in dorsal root ganglion neurons as a processing artifact. The neuron (N) exhibits several small cytoplasmic vacuoles at the cell periphery (arrow), which may be caused by excessive traction applied during tissue collection and processing. A = axons. Asterisks = satellite glial cells. Species: Adult RccHan:Wistar rat. Processing: Aldehyde (not specified) perfusion, Osm postfixation, plastic, TB. Osm = osmium tetroxide, TB = toluidine blue.

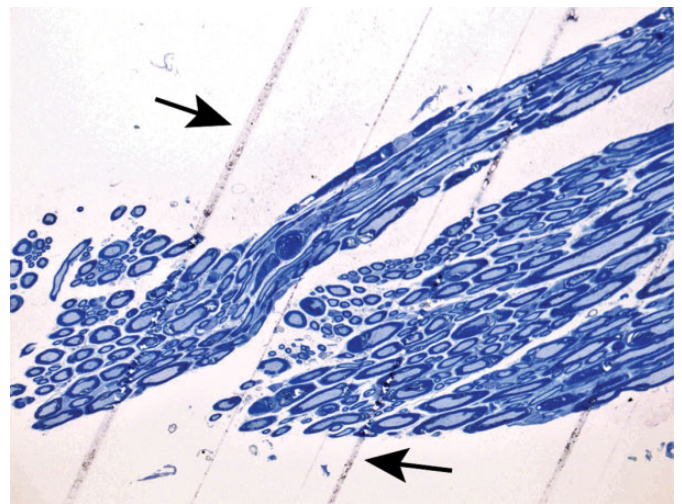


Figure 35. Blade marks as a processing artifact. Multiple parallel lines (arrows) in the cervical spinal nerve resulted from nicks in the cutting edge of the microtome blade. Species: RccHan:Wistar rat. Processing: Aldehyde (not specified) perfusion, Osm postfixation, plastic, TB. Osm = osmium tetroxide, TB = toluidine blue.

or treatment-related effect, since this change is common in control animals of many species.⁵⁷ Linear streaks or tears in sections may result from small nicks in the cutting surface of the microtome blade (Figure 35), but these usually can be discriminated as artifacts with ease. Most processing artifacts are avoidable with sufficient advance planning.

A final set of unique artifacts may be observed when unfixed PNS tissues are flash-frozen to permit immunohistochemical analysis of labile antigens. The main features seen in such cryosections are loss of tissue detail (“smudging” of

nuclear and cytoplasmic features; Figure 36) and/or generation of large spaces within the sections (especially for nerves; Figure 37). In general, the reduced morphologic detail prevents thorough cytoarchitectural evaluation of PNS cryosections, which typically are evaluated for the distribution of molecular signals.

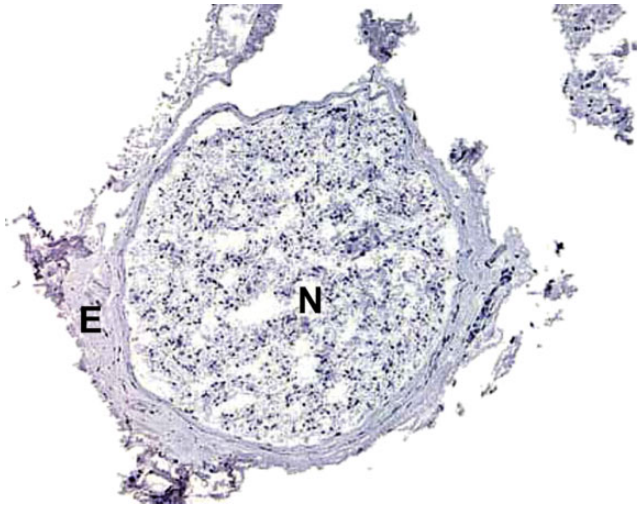


Figure 36. Freeze artifact in a nerve cryosection. Nerve fiber cytoarchitecture is obscured in this 5- μ m-thick frozen section. N = nerve; E = epineurium. Sciatic nerve. Species: Adult RccHan:Wistar rat. Processing: no fixation, optimal cutting temperature (OCT) medium embedding, immunohistochemical procedure with hematoxylin counterstain.



Figure 37. Freeze artifact in a nerve cryosection. Nerve fiber cytoarchitecture is obscured and large, irregular tissue defects (arrows) disrupt the nerve tissue in this 5- μ m-thick frozen section. Sciatic nerve. Species: Adult Crl:Wistar rat. Processing: No fixation, optimal cutting temperature (OCT) medium embedding, H&E. H&E indicates hematoxylin and eosin.

Spontaneous Background Changes

As with other organs, PNS tissues exhibit many incidental background changes (both nonproliferative and proliferative).⁵⁸

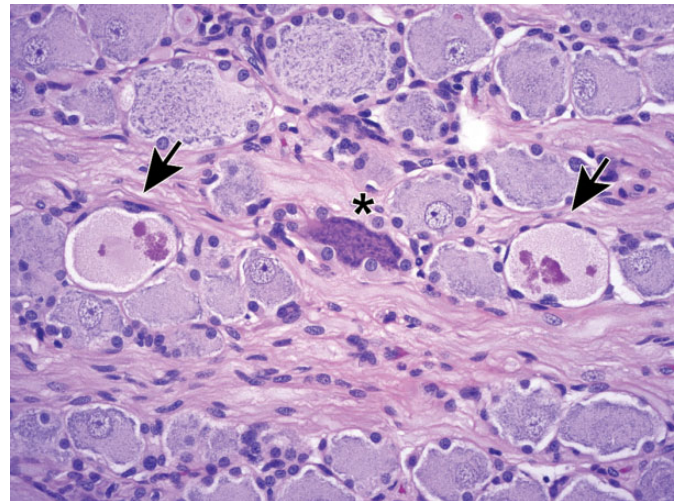


Figure 38. Autophagy of sensory neurons (arrows) in dorsal root ganglia is characterized by loss of a distinct nucleus, condensation of chromatin into irregular hypereosinophilic globules or spicules, and pale-stained cytoplasm containing myriad lightly eosinophilic granules. A "dark neuron" (an artifact, at asterisk) has deeply basophilic nucleoplasm and cytoplasm. Species: Juvenile cynomolgus monkey. Processing: NBF immersion, paraffin, H&E. H&E indicates hematoxylin and eosin; NBF, neutral-buffered 10% formalin.

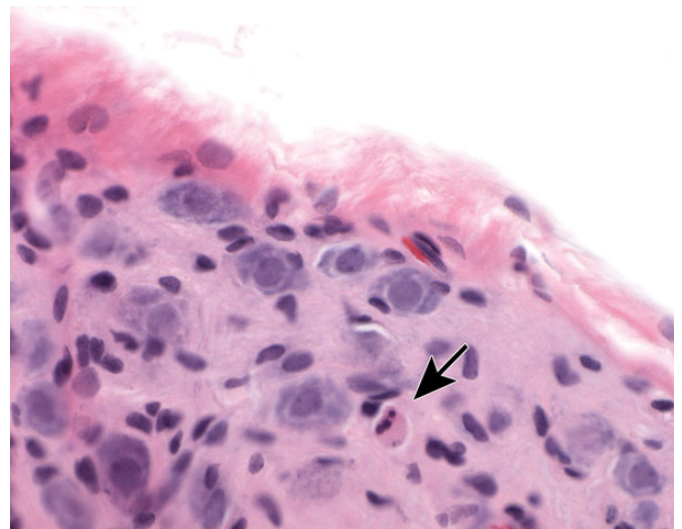


Figure 39. Single-cell necrosis of ganglionic neurons is an occasional finding. Dead neurons (arrow) appear as shrunken cells with condensed, dark, sometimes fragmented, basophilic nuclei and deeply eosinophilic cytoplasm (termed "red dead" cells). This finding can occur in controls and may be exacerbated by test articles. Mesenteric (parasympathetic) ganglion. Species: Young adult Wistar rat. Processing: NBF immersion, paraffin, H&E. H&E indicates hematoxylin and eosin; NBF, neutral-buffered 10% formalin.

These changes may increase in incidence and/or severity with age. Importantly, these findings are not induced by test article administration, but their incidence and/or severity may be exacerbated by exposure to certain test articles.

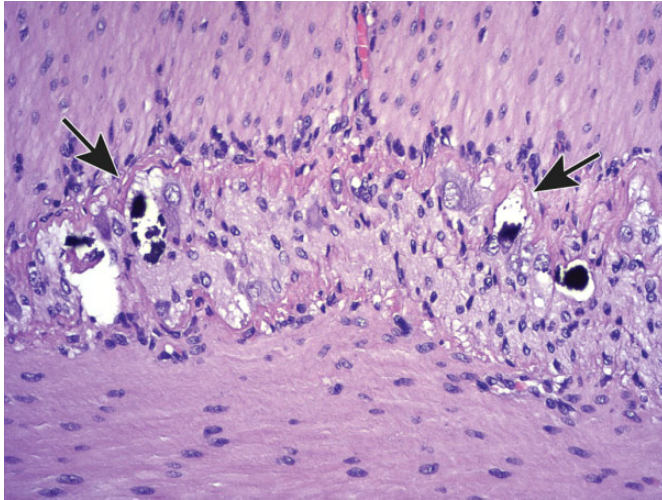


Figure 40. Mineralization of neurons (arrows) in the jejunal myenteric plexus. This change may occur in the absence of other changes. Species: Adult, female Beagle dog. Processing: NBF immersion, paraffin, H&E. H&E indicates hematoxylin and eosin; NBF, neutral-buffered 10% formalin.

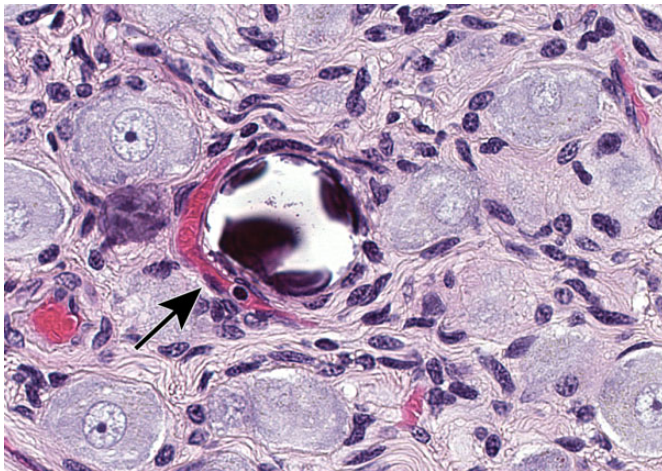


Figure 41. Mineralization of neurons (arrow) in the superior cervical ganglion. Species: Juvenile cynomolgus monkey. Processing: NBF immersion, paraffin, H&E. H&E indicates hematoxylin and eosin; NBF, neutral-buffered 10% formalin.

Ganglia exhibit many spontaneous background changes. One hallmark finding is sensory neuron autophagy (Figure 38).⁵⁹ Autophagic cells have hypereosinophilic, condensed, residual chromatin (resulting from nuclear loss) and pale eosinophilic, granular cytoplasm. These cells may be seen in any species but are particularly common in DRGs of nonhuman primates (including naive controls); in most cases, multiple DRGs are involved in an affected individual. Single-cell necrosis is an occasional finding in ganglia (Figure 39). Ganglionic neurons may be mineralized (Figures 40 and 41) or contain neuromelanin (Figure 42), a finely stippled brown cytoplasmic pigment with no known pathological significance. Increased cellularity due to

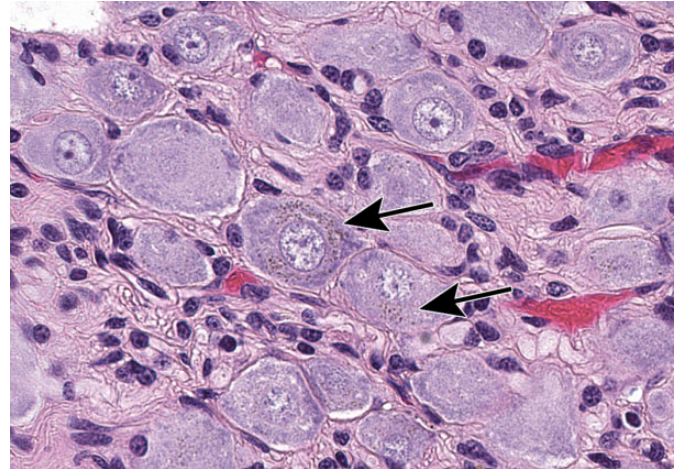


Figure 42. Neuromelanin in neurons in the superior cervical ganglion appears as finely stippled, brown cytoplasmic pigment (arrow). This change is without pathologic significance and occurs most commonly in nonhuman primates and C57BL/6 mice. Species: Adult cynomolgus monkey. Processing: NBF immersion, paraffin, H&E. H&E indicates hematoxylin and eosin; NBF, neutral-buffered 10% formalin.

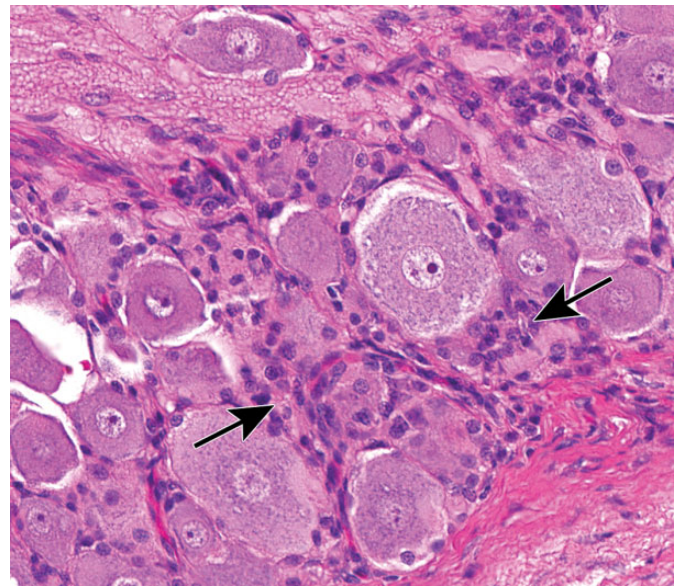


Figure 43. Increased cellularity due to satellite glial cell hyperplasia in a dorsal root ganglion (arrows) is characterized by increased numbers of round to oval, pale basophilic nuclei among neurons. Species: Young adult Beagle dog. Processing: NBF immersion, paraffin, H&E. H&E indicates hematoxylin and eosin; NBF, neutral-buffered 10% formalin.

hyperplasia of satellite cells among neurons (sometimes called Nageotte nodules when associated with neuronal loss;⁶⁰ Figure 43) or Schwann cells within intraganglionic nerve fiber bundles (Figure 44) are observed with variable frequency. In addition, accumulation of mononuclear cells (typically lymphocytes with a few macrophages; Figure 45) or mixed leukocytes (mainly lymphocytes, macrophages, and neutrophils; Figure 46) may occur around neurons. Satellite cell hyperplasia often develops

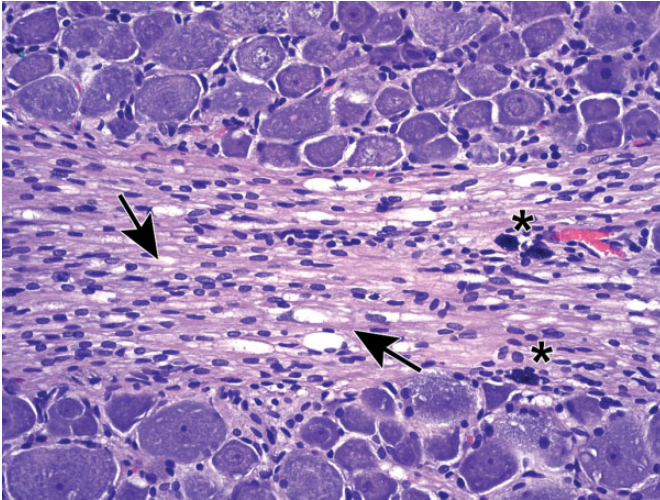


Figure 44. Increased cellularity due to Schwann cell hyperplasia (arrows) within the nerve fiber fascicles coursing through the L₄ dorsal root ganglion. This change features many dark basophilic spindle cell nuclei. Multiple dark basophilic mast cells (asterisks) are seen, which is a common observation in PNS tissues. Species: Adult Sprague-Dawley rat. Processing: NBF immersion, paraffin, H&E. H&E indicates hematoxylin and eosin; NBF, neutral-buffered 10% formalin.

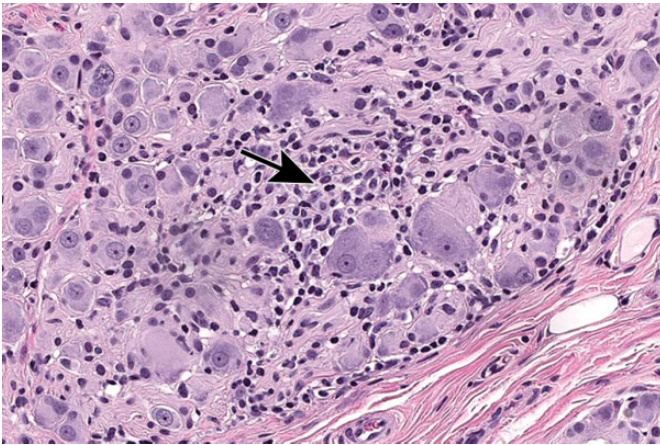


Figure 45. Increased cellularity due to mononuclear cell infiltration with some satellite glial cell proliferation in a parasympathetic ganglion in the seminal vesicle. Infiltration is diagnosed when migrating leukocytes are not associated with parenchymal damage. Mononuclear cells—mainly lymphocytes (small, dark basophilic, round nuclei) with some macrophages (larger, pale basophilic, oval nuclei with pale cytoplasm)—can be differentiated from satellite glial cells (small, pale basophilic, round nuclei) at higher magnifications. Species: Adult, male cynomolgus monkey. Processing: NBF immersion, paraffin, H&E. H&E indicates hematoxylin and eosin; NBF, neutral-buffered 10% formalin.

in association with mononuclear cell infiltration (ie, leukocyte influx without parenchymal injury) or inflammation (leukocyte entry with damage to parenchymal cells). Lamellar bodies are small foci of fibrous tissue and myelin arranged in concentric rings around a central glial cell (Figure 47). In general, such

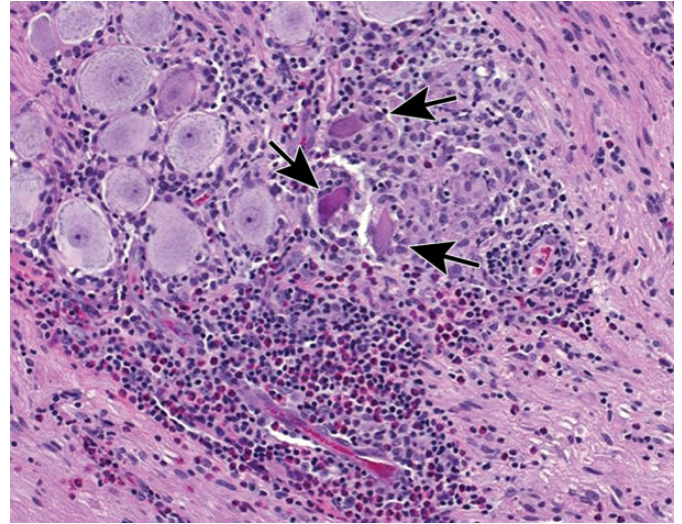


Figure 46. Mixed cell inflammation and neuronal necrosis in the trigeminal ganglion. Inflammation is diagnosed when the migrating leukocytes are associated with damage to the PNS parenchyma, in this case neuronal death (arrows denote “red dead” cells). Mixed cell lesions include lymphocytes, macrophages, and granulocytes (neutrophils and/or eosinophils) and often are accompanied by satellite glial cell hyperplasia. This spectrum of changes can be caused by natural viral infections (eg, cytomegalovirus, herpes B virus) and some viral gene therapy vectors, and lesions may be exacerbated by concurrent immunosuppressive therapies. Species: Juvenile, female cynomolgus monkey. Processing: NBF immersion, paraffin, H&E. H&E indicates hematoxylin and eosin; NBF, neutral-buffered 10% formalin; PNS, peripheral nervous system.

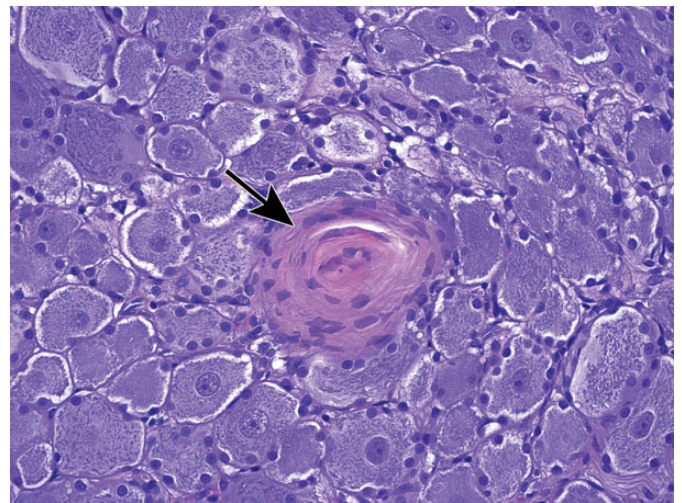


Figure 47. Lamellar body in the L₅ dorsal root ganglion (arrow). This change features concentric layers of fibrous connective tissue (with fibroblasts) and myelin surrounding a central satellite glial cell. This finding has no pathological significance. Species: Juvenile cynomolgus monkey. Processing: NBF immersion, paraffin, H&E. H&E indicates hematoxylin and eosin; NBF, neutral-buffered 10% formalin.

ganglionic changes should be of minimal severity to be considered incidental, spontaneous findings.

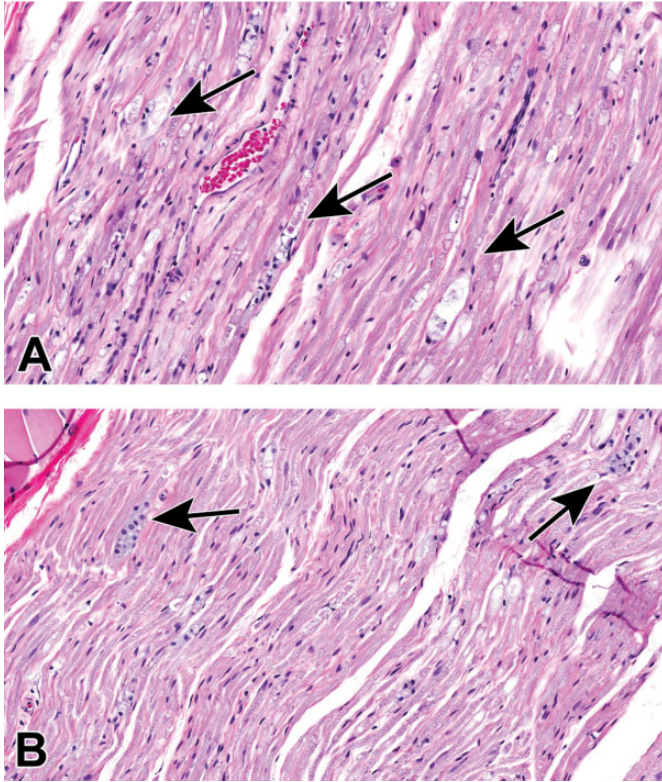


Figure 48. Nerve fiber degeneration in the sciatic nerve. A, Affected nerve fibers are reduced to granular eosinophilic to amphiphilic debris (arrows) held within intact basement membranes. B, In areas with multiple affected fibers, small clusters of macrophages (arrows) scavenge axonal and myelin debris. Degeneration of isolated nerve fibers (one to three per section in controls animals) is a frequent background change in all species that can increase in incidence and severity with age. Species: Young adult Wistar rat. Processing: NBF immersion, paraffin, H&E. H&E indicates hematoxylin and eosin; NBF, neutral-buffered 10% formalin.

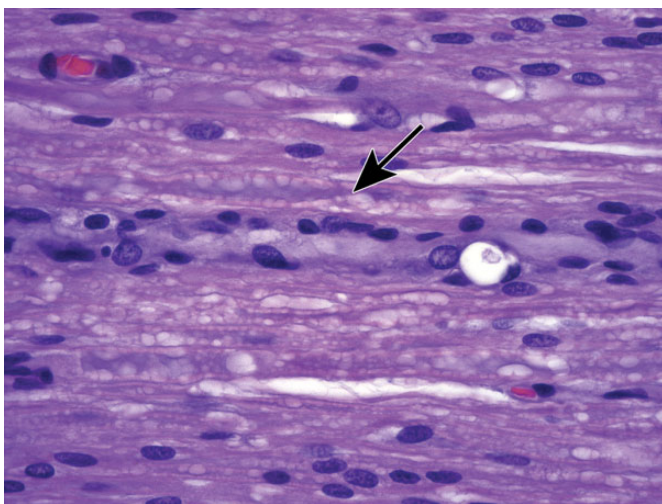


Figure 49. Nerve fiber degeneration and regeneration bands (or bands of Bünger) in the sciatic nerve. Degeneration is evident as a single nerve fiber with a large, round cavity containing a small raft of eosinophilic debris. The regeneration band (arrow), which consists of a narrow column of proliferating Schwann cells, will serve as a substrate to support regrowth of the regenerating axon. Species: Young adult Sprague-Dawley rat. Processing: NBF immersion, paraffin, H&E. H&E indicates hematoxylin and eosin; NBF, neutral-buffered 10% formalin.



Figure 50. Mononuclear cell infiltration in the sciatic nerve. These foci (arrow) contain lymphocytes with occasional macrophages, typically form around a small arteriole or capillary, and are not associated with damage to adjacent nerve fibers. Species: Juvenile cynomolgus monkey. Processing: NBF immersion, paraffin, H&E. H&E indicates hematoxylin and eosin; NBF, neutral-buffered 10% formalin.



Figure 51. Matrix accumulation adjacent to a lumbar spinal nerve root. The paucicellular material may be normal connective tissue and can be seen within the body of spinal nerve roots as a function of cut artifact. Species: Adult, female Rhesus monkey. Processing: NBF immersion, paraffin, H&E. H&E indicates hematoxylin and eosin; NBF, neutral-buffered 10% formalin.

Nerves also display many spontaneous background findings. The most common lesion is nerve fiber degeneration (Figure 48), which may be observed in any nerve. This finding often is visible in untreated and vehicle-treated control animals as 1 to 3 affected fibers. The incidence of nerve fiber degeneration as a

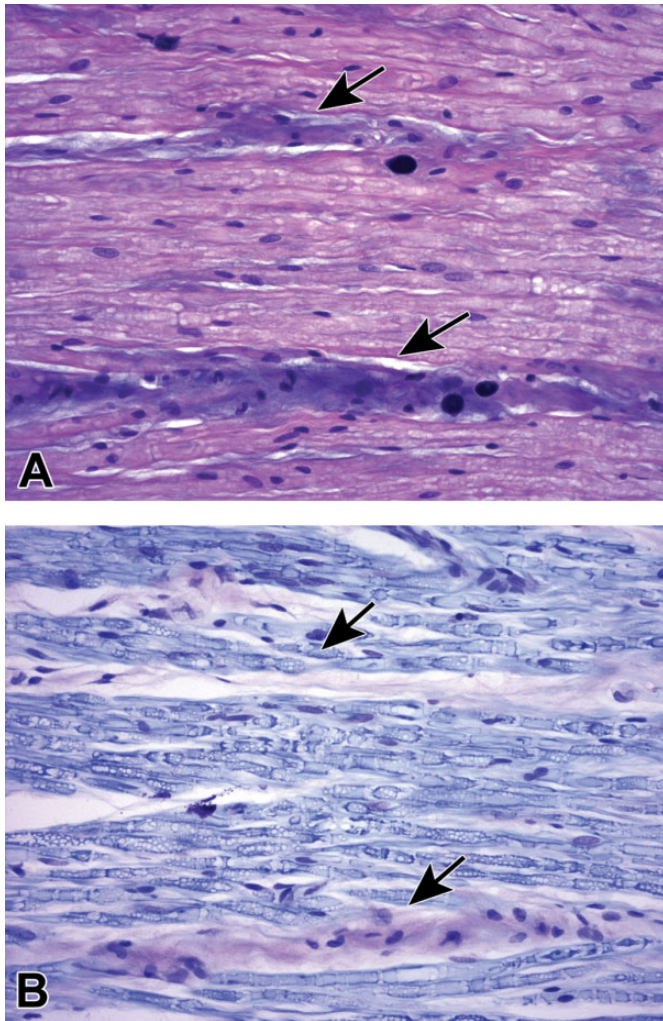


Figure 52. Matrix accumulation in the proximal sciatic nerve associated with the L₄ lumbar dorsal root ganglion. A, In H&E-stained sections, this material occurs as isolated or coalescing, linear bands of homogenous blue-purple matrix containing occasional plump spindle cells (arrows). B, In LFB-stained sections, matrix bands are pale pink (arrows). Species: Young adult Sprague-Dawley rat. Processing: NBF immersion, paraffin. H&E indicates hematoxylin and eosin; NBF, neutral-buffered 10% formalin; LFB, Luxol fast blue.

background change ranges from 1% to over 20% and increases substantially with age.^{61–63} Rodents are much more affected than nonrodents. Even young adult rats may exhibit high spontaneous incidences. In dogs and monkeys, the background incidences are very low. In general, nerve fiber disintegration may be so advanced that it is not clear whether the initial effect was in the axon (ie, axonal degeneration) or the adjacent Schwann cells (ie, demyelination) when evaluating paraffin-embedded, H&E-stained sections. In most cases, nerve fiber degeneration results from primary destruction of the axon (ie, “axonal degeneration”), but in some cases the initial lesion is primary damage to myelin sheaths (ie, “demyelination”).¹ These changes may be differentiated using special stains designed to detect axonal or myelin elements (Figure 16).⁸ Occasionally, a degenerating

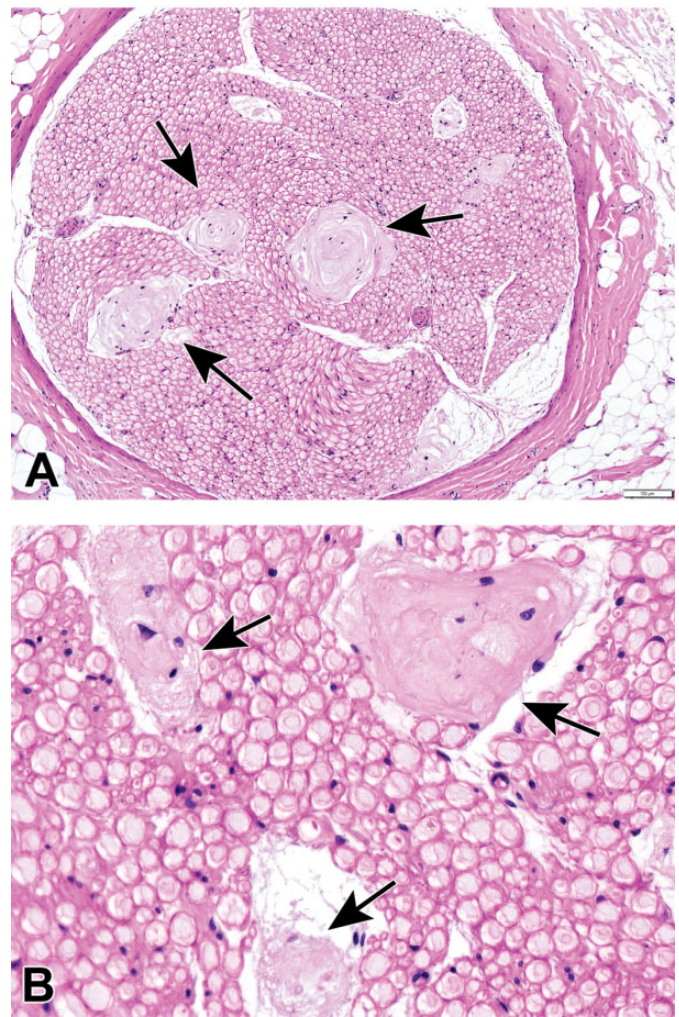


Figure 53. Renaut bodies (arrows in A and B) are subperineurial accumulations of elongate, loosely whorled, mucin-rich, cell-poor connective tissue. These findings usually occur in sensorimotor nerves as a potential consequence of nerve compression. Their incidence and severity both may increase (as an indirect effect) if test article administration leads to prolonged recumbency. Sciatic nerve. Species: Young adult Beagle dog. Processing: NBF immersion, paraffin, H&E. H&E indicates hematoxylin and eosin; NBF, neutral-buffered 10% formalin.

nerve fiber is accompanied by a linear column of proliferating and hypertrophic Schwann cells which forms a permissive substrate through which regenerating axons may regrow (termed “regeneration bands” or bands of Büngner; Figures 49).⁶⁴ Small foci of mononuclear cell infiltration (Figure 50) are an occasional finding in myelinated nerves, especially in nonhuman primates. Accumulation of cell-poor matrix (Figures 51 and 52) may be seen occasionally in any nerve but is most common in the nerve fascicles near or in DRGs. The significance of such matrix foci is not known. In contrast, Renaut bodies are elongated collections of mucin-rich, cell-poor, laminated connective tissue which occur within nerves in association with the perineurium. These bodies occur most commonly in sensorimotor nerves (Figure 53) but can develop in

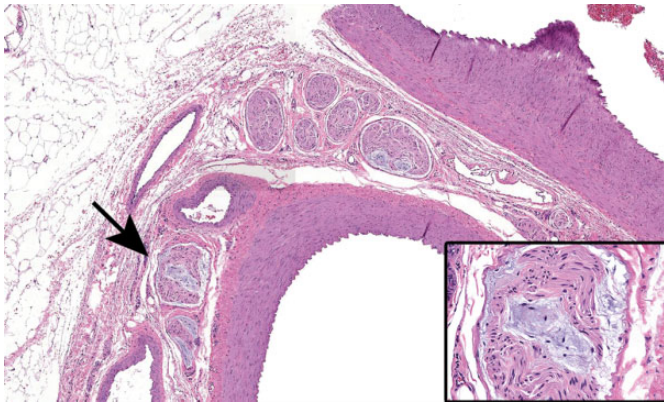


Figure 54. Renaut bodies may occur in autonomic nerves of dogs, but often are missed since these sites are not sampled routinely in general toxicity studies. Vagus nerve (cranial nerve X) branches (arrow) associated with mesenteric arteries. Species: 18-month-old Beagle dog. Processing: NBF immersion, paraffin, H&E. H&E indicates hematoxylin and eosin; NBF, neutral-buffered 10% formalin.

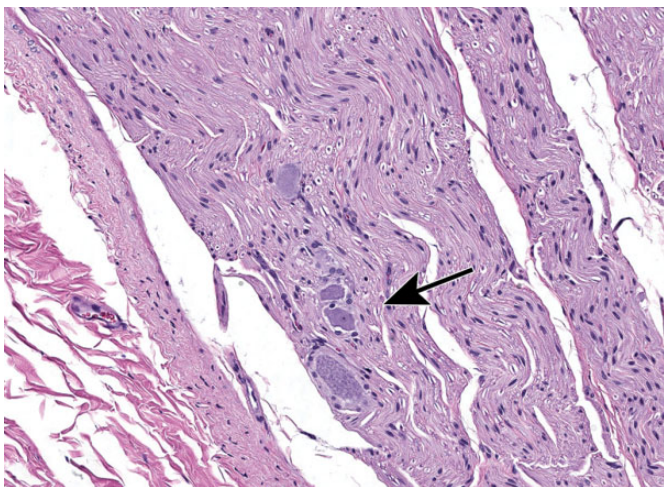


Figure 55. Ectopic neurons (arrow) in the vagus nerve (cranial nerve X) near the caudal vagal ("nodose") ganglion. Occasional isolated neurons may be present in nerve trunks, especially in the autonomic system. Species: Young adult, male Beagle dog. Processing: NBF immersion, paraffin, H&E. H&E indicates hematoxylin and eosin; NBF, neutral-buffered 10% formalin

autonomic nerves (Figure 54). Renaut bodies may be formed in areas of nerve compression and can affect a large proportion of animals (including multiple controls) in some toxicity studies.^{65,66} Finally, isolated neurons or small neuron clusters may be observed in many nerves in proximity to ganglia (Figures 12 and 55). These cells may represent either ectopic ganglionic neurons (Figure 55) or autonomic neurons (Figure 12). The presence of these neurons is not known to have adverse implications with respect to PNS function.

Proliferative findings in the PNS also can develop as spontaneous background changes.⁶⁷⁻⁷⁰ Neoplasms arising from PNS cells originate almost entirely from glial cells since

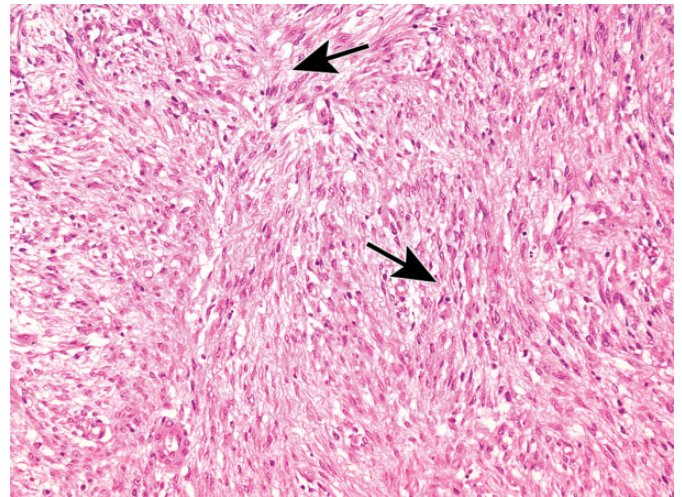


Figure 56. Malignant schwannoma in the skin. This Schwann cell-derived neoplasm is characterized by spindle cells with indistinct cell margins and oval to round, hyperchromatic nuclei, often arranged in whorls (Verocay bodies) and palisades. Cell organization exhibits 2 patterns, Antoni type A (densely packed cells [arrows]) and/or Antoni type B (loosely packed cells with pseudocystic spaces and edema). Species: Adult RccHan:Wistar rat. Processing: NBF immersion, paraffin, H&E. H&E indicates hematoxylin and eosin; NBF, neutral-buffered 10% formalin.

ganglionic neurons represent terminally differentiated (ie, nonproliferating) cells. Schwann cell tumors, or schwannomas (Figures 56 and 57), may be benign or malignant.⁷¹ Common sites for schwannomas include the heart ("endocardial schwannoma"), nerve plexuses, and skin. Paragangliomas (Figure 58) are rare tumors of autonomic ganglia that are composed of round, catecholamine-producing round cells. These neoplasms closely resemble pheochromocytomas (ie, adrenal medullary tumors, where the adrenal medulla functions as an autonomic ganglion). Test articles may rarely increase the incidence of PNS tumors.⁶⁷⁻⁷⁰

Test Article–Related Findings

With respect to PNS neurotoxicity, particular care must be given to distinguish whether the primary lesions result from damage to ganglionic neurons, axons, or myelin.^{1,72,73} Four categories of primary nonproliferative PNS lesions may be produced by neurotoxic exposures: primary neuronopathies, primary axonopathies, primary myelinopathies, and neuroaxonal dystrophy. In addition, certain PNS neurotoxicants may induce proliferative lesions. The susceptibility to toxicant-induced damage can be affected by genetic factors.⁷⁴ These same changes occur sporadically as background findings, typically in older animals.

Primary neuronopathies (also called *ganglionopathies*) feature degenerating neurons, with or without satellite cell hyperplasia or leukocyte infiltration. Affected neurons exhibit various combinations of swelling and/or vacuolation (ie, hydropic degeneration; Figures 59 and 60), often with chromatolysis (ie, dissolution of rough endoplasmic reticulum [termed

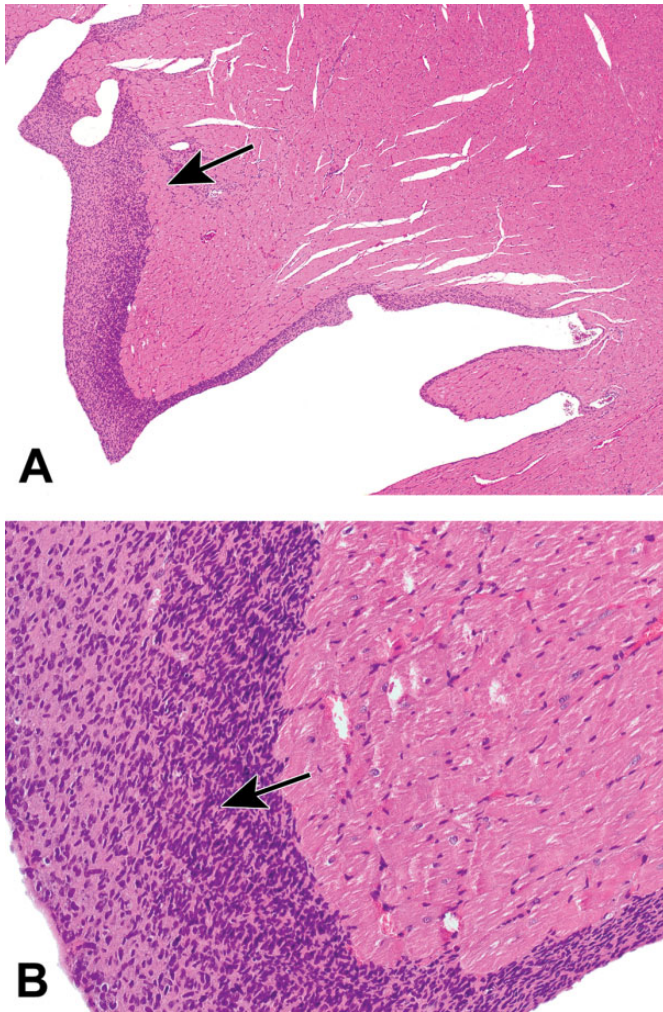


Figure 57. Endocardial schwannoma in the heart. A and B, The endocardium is focally expanded by long parallel bundles of neoplastic spindle cells with hyperchromatic, elongated nuclei; eosinophilic cytoplasm; and indistinct cell borders (arrows). These tumors sometime exhibit Verocay bodies (collections of fusiform cells arranged in whorls, herringbones, or palisades). Species: Adult RccHan:Wistar rat. Processing: NBF immersion, paraffin, H&E. H&E indicates hematoxylin and eosin; NBF, neutral-buffered 10% formalin.

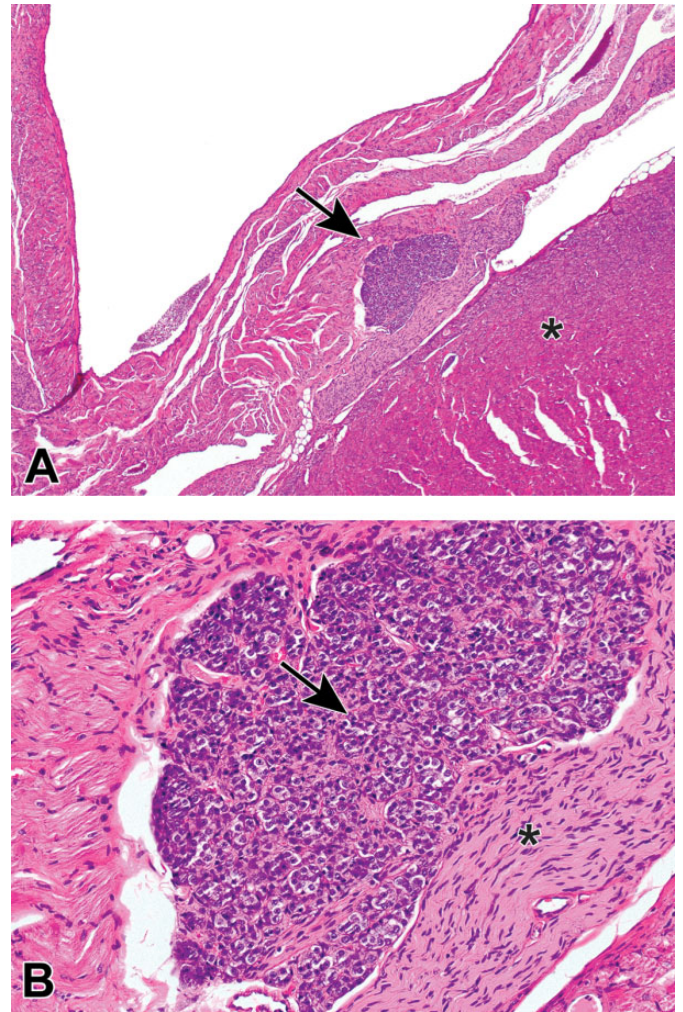


Figure 58. Paraganglioma in a parasympathetic ganglion at the heart base. A, A well-demarcated mass (arrow) is evident in the aortic wall. Asterisk = wall of the left ventricle. B, The tumor is composed of well-differentiated, round, neoplastic neuroendocrine cells (arrow) arranged in clusters. Asterisk = nerve fibers derived from non-neoplastic ganglionic neurons are surrounding neoplastic cells. Species: Hsd:SD Harlan rat. Processing: NBF immersion, paraffin, H&E. H&E indicates hematoxylin and eosin; NBF, neutral-buffered 10% formalin.

Nissl substance] needed to support increased protein synthesis; Figures 61 and 62). In some cases, degenerating neurons can develop accumulations of a test article, such as phospholipidosis, associated with administration of cationic amphiphilic drugs (Figure 61). Degeneration of ganglionic neurons may progress to frank neuronal necrosis, especially in association with intense inflammation (Figure 62; see also Figure 46). Confidently distinguishing neuron degeneration from neuron necrosis may not always be possible in ganglionic neurons.

Primary axonopathies are characterized by swollen, disintegrating, or missing axons (Figures 63 and 64), in some cases surrounded by normal or increased numbers of intact Schwann cells that participate in nerve fiber fragmentation and removal. A central-peripheral distal (“dying back”) axonopathy, the most common PNS neurotoxic lesion,²⁹ is characterized by degenerative lesions that develop first in distal nerve branches (ie, closer to axon terminals) and progress over time to also

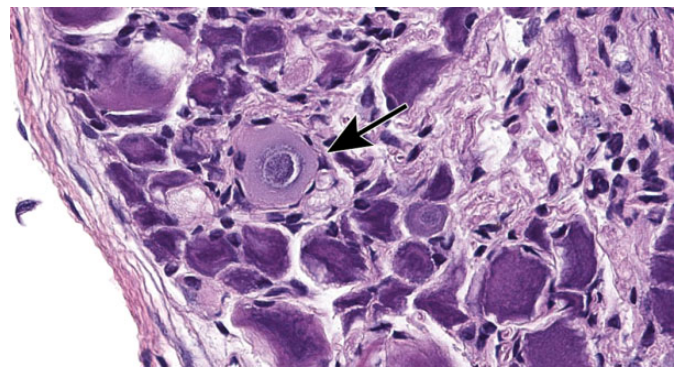


Figure 59. Neuron degeneration in the L₄ lumbar dorsal root ganglion following administration of an antineoplastic drug. The affected cell (arrow) is slightly swollen and exhibits a clear halo around a basophilic nucleus. Surrounding neurons are shrunken and have uniformly dark basophilic nuclei (barely visible in some cells) and cytoplasm (ie, “dark neuron” artifact). Species: Adult Wistar rat. Processing: NBF immersion, paraffin, H&E.

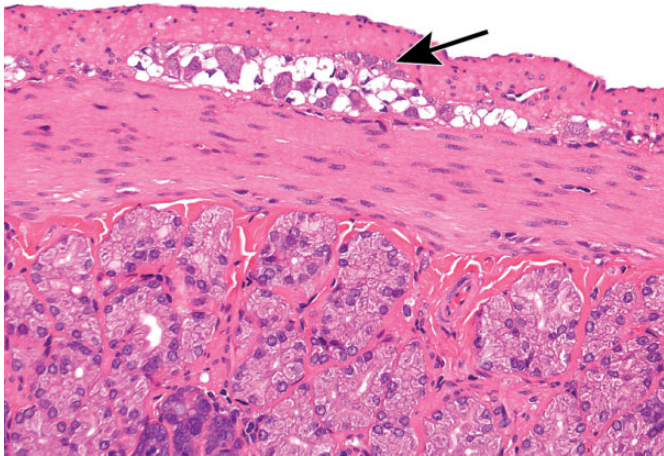


Figure 60. Neuron degeneration in the duodenal myenteric plexus following treatment with a neuroactive test article. Neuron cell bodies in all enteric ganglia exhibit swelling and diffusely clear cytoplasm (i.e., 'hydropic degeneration'). Species: Young adult RccHan:Wistar rat. Processing: NBF immersion, paraffin, H&E. H&E indicates hematoxylin and eosin; NBF, neutral-buffered 10% formalin.

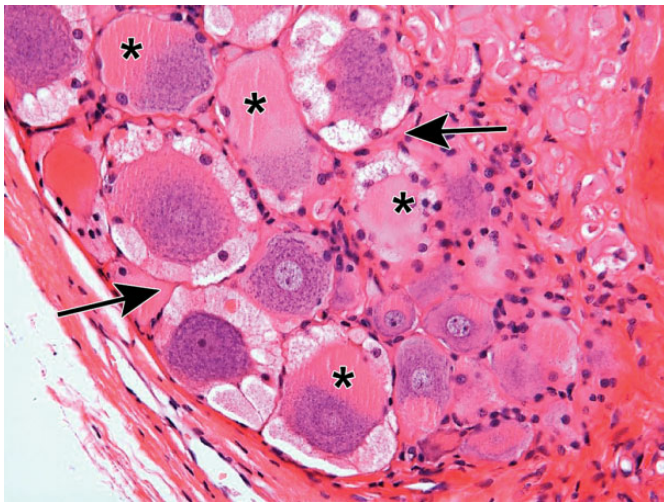


Figure 61. Neuron phospholipidosis (arrows) and chromatolysis (asterisks) in the dorsal root ganglion following treatment for 52 weeks with an antibiotic. Phospholipidosis (confirmed by electron microscopy) is characterized by neurons and satellite glial cells exhibiting massive cytoplasmic extension due to accumulation of large vacuoles filled with amorphous, eosinophilic material. Partial chromatolysis is characterized by dissolution of Nissl substance (ie, pallor of the cytoplasm) and eccentric nuclei. Species: Adult Beagle dog. Processing: NBF immersion, paraffin, H&E. H&E indicates hematoxylin and eosin; NBF, neutral-buffered 10% formalin.

affect more proximal portions of the nerve fibers. The presence of primary axonal damage may lead to secondary chromatolysis (termed the "axonal reaction") of the ganglionic neurons (Figure 65). Since proteins to repair the axon extremities are generated mainly in the cell soma, chromatolysis (ie,

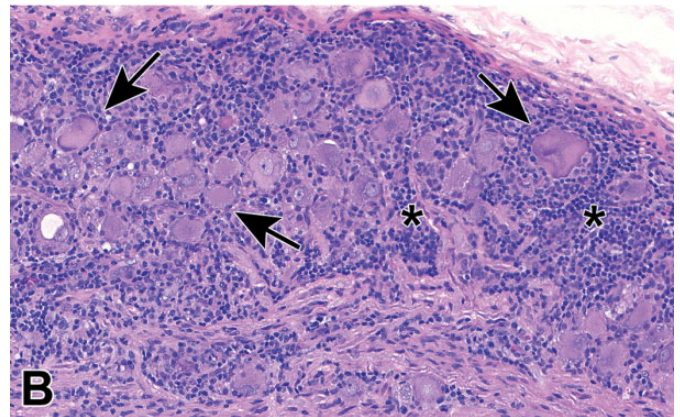
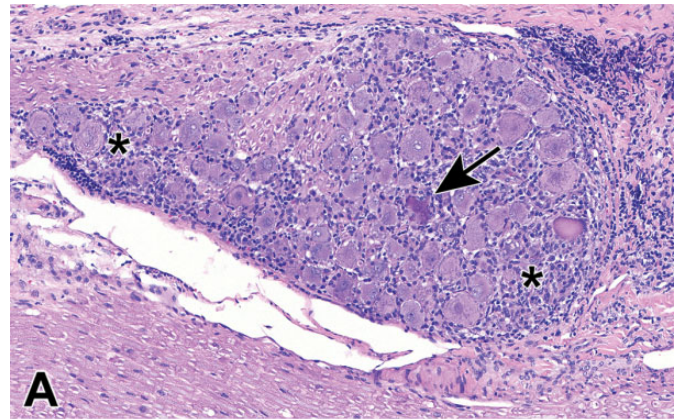


Figure 62. Inflammation and neuron degeneration/necrosis in a lumbar dorsal root ganglion associated with intrathecal injection of an unspecified gene therapy vector. A and B, The reaction includes early neuronal degeneration with later neuron necrosis (arrows) associated with an influx of mononuclear cells (asterisks). The variable morphology of damaged neurons often precludes definitive diagnosis of degeneration versus necrosis. Foci of proliferating satellite glial cells (termed Nageotte nodules) fill the gaps left by loss of necrotic neurons. Species: Juvenile cynomolgus monkey. Processing: NBF immersion, paraffin, H&E. H&E indicates hematoxylin and eosin; NBF, neutral-buffered 10% formalin.

dissolution of dark basophilic Nissl substance granules to release aggregated ribosomes) is a prerequisite for the enhanced protein synthesis needed to replace a damaged axon. Primary axonal damage may lead to secondary myelin degeneration resulting from the loss of axon-derived trophic factors needed to maintain Schwann cells.

Primary myelinopathies result from initial damage to Schwann cells. These conditions appear in sections as intact axons surrounded by thin or absent myelin sheaths (Figure 66). In some instances, the myelin lamellae are split and widely separated due to the accumulation of fluid (Figure 66). Cellularity often is increased within the affected tissue due to proliferation of remyelinating Schwann cells (Figure 67) and/or accumulation of macrophages (for removal of nerve fiber debris). Recovery from primary myelinopathies is associated with increases in Schwann cell nuclei because newly formed Schwann cells cover less axonal area than original Schwann cells. Accordingly,

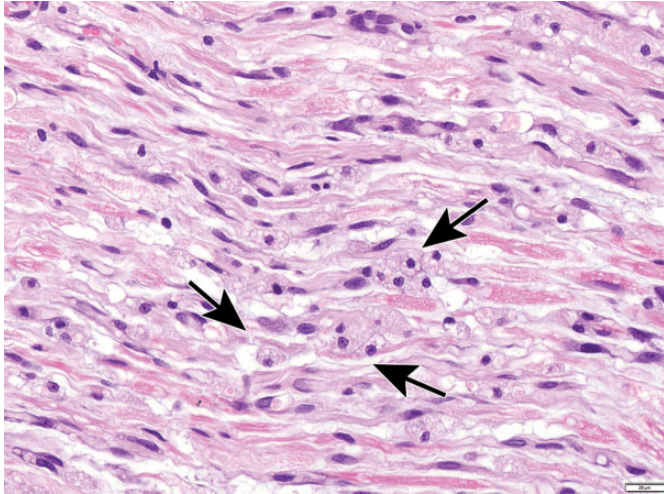


Figure 63. Nerve fiber degeneration in the sciatic nerve treated for 28 days with an unspecified xenobiotic. Affected nerve fibers exhibit eosinophilic debris from fragmentation of both axons and myelin as well as numerous large, foamy macrophages that are scavenging the debris (arrows). Species: Adult rat (strain unspecified). Processing: NBF immersion, paraffin, H&E. H&E indicates hematoxylin and eosin; NBF, neutral-buffered 10% formalin.

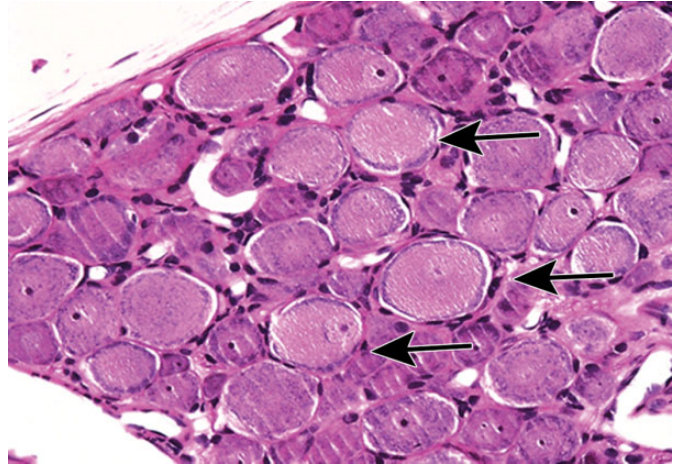


Figure 65. Chromatolysis in dorsal root ganglion neurons secondary to a primary axonopathy (termed the “axonal reaction”) following 15 days of acrylamide treatment. Prominently affected cells (arrows) are enlarged and have abundant pale eosinophilic cytoplasm at their centers with small quantities of dark basophilic Nissl substance located at the cell periphery. Species: Adult rat (strain unspecified). Processing: NBF immersion, paraffin, H&E. H&E indicates hematoxylin and eosin; NBF, neutral-buffered 10% formalin.

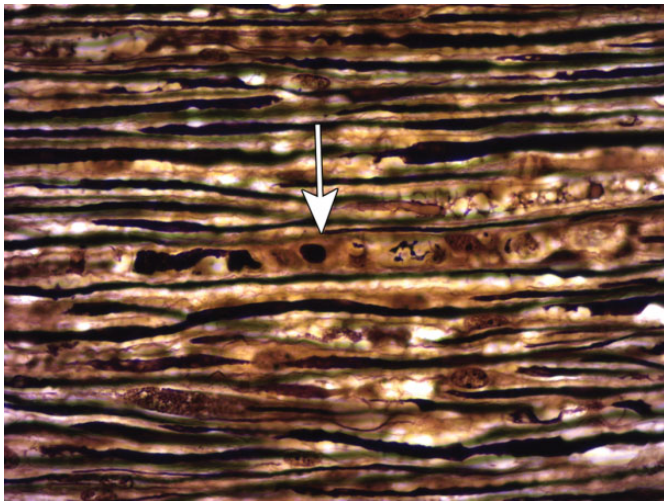


Figure 64. Nerve fiber degeneration in the L₄ lumbar dorsal spinal nerve root following treatment with an unspecified xenobiotic. Affected nerve fibers (arrow) exhibit irregular argyrophilic (black) axonal fragments associated with columns of pale-stained Schwann cell nuclei (ie, regeneration bands). Species: Young adult Sprague-Dawley rat. Processing: NBF immersion, paraffin, Bielschowsky silver stain. H&E indicates hematoxylin and eosin; NBF, neutral-buffered 10% formalin.

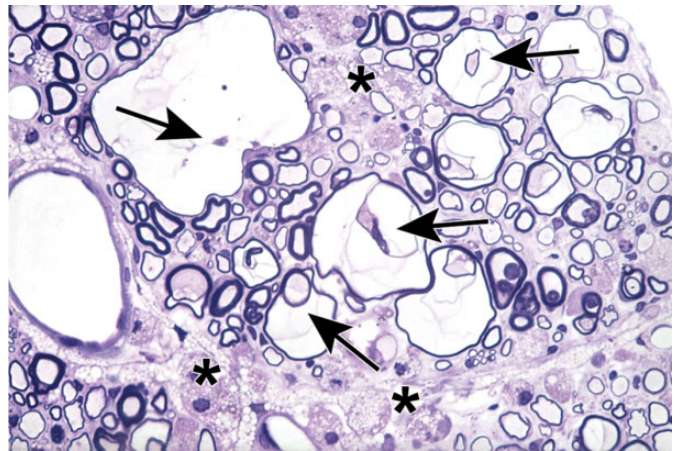


Figure 66. Primary demyelination in a spinal nerve root. Affected nerve fibers have central axons (arrows) surrounded by large spaces resulting from intramyelinic fluid accumulation and severe myelin thinning. The interstitial spaces between nerve fibers contain many plump foamy macrophages (asterisks). Species: Aged (30-month-old), male, Sprague-Dawley rat. Processing: Glut perfusion, Osm postfixation, plastic, TB. Glut = glutaraldehyde, Osm = osmium tetroxide, TB = toluidine blue.

remyelinated nerves have more nodes of Ranvier and a measurably decreased ability to conduct nerve impulses.

Finally, *neuroaxonal dystrophy* is characterized by axonal swelling (Figure 68) along with subcellular abnormalities such as accumulations of cytoskeletal elements, tubulovesicular profiles, and/or granular/membranous bodies as well as distorted mitochondria. Such axonal swellings

(often termed “spheroids”) arise either in nerve terminals from disrupted recycling and retrograde transport leading to organelle accumulation or else from disrupted anterograde transport leading to accumulation of cross-linked cytoskeletal filaments proximal to nodes of Ranvier (eg, in γ -diketone neuropathy). Control animals (especially older ones) of all species occasionally exhibit a few degenerating or dystrophic nerve fibers as an incidental background

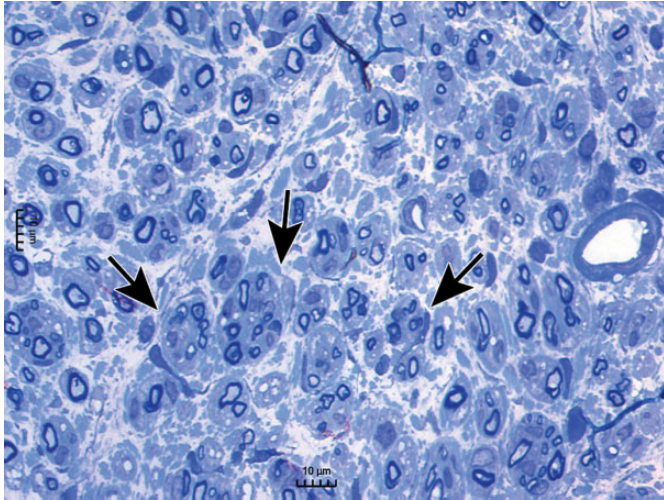


Figure 67. Laminar accumulation of Schwann cells (“hypertrophic neuropathy”) in the sciatic nerve. Affected nerve fibers (arrows) exhibit concentric layers (termed “onion bulbs”) composed of Schwann cells mixed with collagen that result from repeated cycles of myelin degeneration and regeneration. Axons are intact, but the thickness of myelin sheaths is variable and often quite thin. Species: Juvenile cynomolgus monkey. Processing: Aldehyde (not specified) perfusion, Osm postfixation, plastic, TB. Osm = osmium tetroxide, TB = toluidine blue.

finding. In contrast, genuine neurotoxic lesions typically affect multiple nerve fibers.

In the case of those neurotoxic lesions that can resolve, complete restoration of nonproliferative PNS neurotoxic lesions requires an extended period of time. For example, chickens treated with an organophosphorus ester exhibit partial but not complete recovery of nerve structures at 7 weeks post-exposure but nearly complete recovery by 9 weeks postexposure.⁷⁵ In rats with a traumatic (“crush”) injury to the median nerve, the normal number of nerve fibers is restored by 24 weeks, but axon diameters, nerve fiber diameters, and myelin thicknesses remain diminished.⁷⁶ Visible evidence of PNS restoration might or might not become evident during standard recovery periods in typical animal toxicity studies (ie, one-third to one-half of the time spent on treatment). The rate of axonal regeneration is limited to the pace of slow anterograde axonal transport (ie, approximately 0.5-1 mm/d⁷⁷), which equates to axon regrowth of approximately 1.5 to 3 cm during a 4-week recovery period. The degree of PNS regeneration is likely to be underestimated by light microscopic evaluation.⁷⁸

An adequate evaluation of nonproliferative PNS neurotoxicity and recovery during animal toxicity studies requires that the spinal cord also be evaluated. In addition to these cell type-specific changes in routine nerve sections, axonopathies and myelinopathies affecting spinal nerves also may be differentiated by the patterns of corresponding nerve fiber damage in the spinal cord because many fiber tracts in the spinal cord white matter carry axons from PNS neurons (Figure 69).²⁹ Therefore, evaluation of nonproliferative PNS neurotoxicity and recovery during animal toxicity studies requires that the

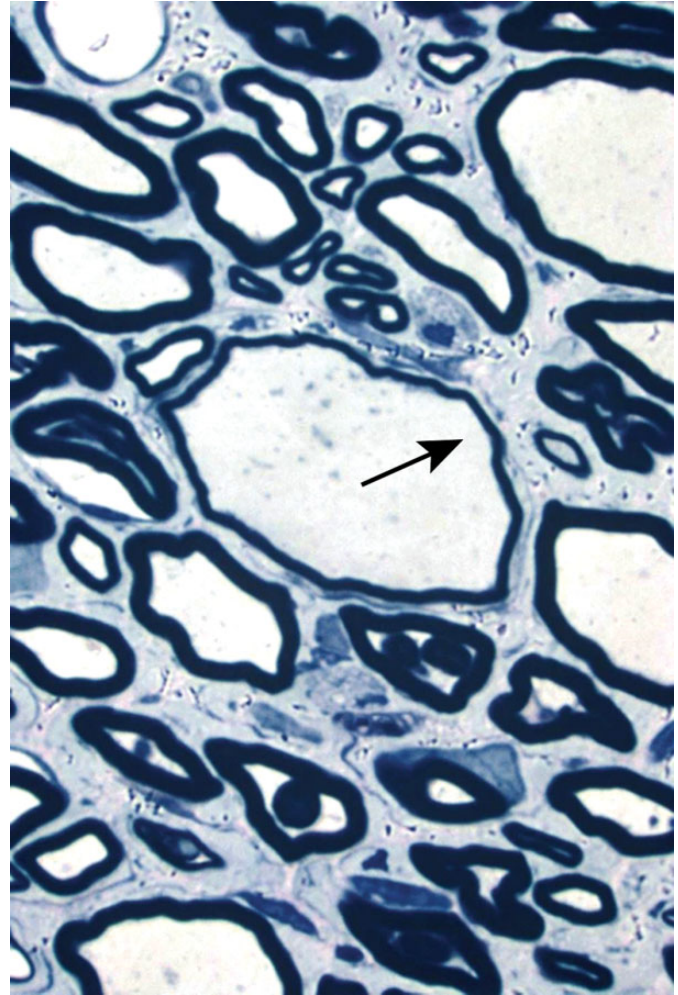


Figure 68. Neuroaxonal dystrophy (“spheroids”) in the sciatic nerve following treatment with *N*-hexane (a γ -diketone chemical). Affected nerve fibers have variably sized but often very large, pale-stained axons with thin myelin sheaths (shown here via arrows). Distended axons contain subcellular anomalies such as accumulations of cytoskeletal filaments, tubulovesicular profiles, and/or granular/membranous bodies as well as distorted mitochondria (not evident in light microscopic preparations). Species: Adult rat (strain unspecified). Processing: Glut perfusion, Osm postfixation, plastic, TB. Glut = glutaraldehyde, Osm = osmium tetroxide, TB = toluidine blue.

spinal cord also be evaluated. At minimum, the spinal cord should be examined using transverse and oblique (or longitudinal) sections through the cervical and lumbar divisions, as described previously.^{8,79} In particular, the C₁ level of the cervical spinal cord is near the termini of the cuneate and gracile fascicles, which are the key sensory tracts in the white matter of the dorsal (posterior [in bipeds]) columns. The actual level at which samples are taken may be adjusted to evaluate potential regions of damage as suggested by in-life neurological signs. Because the spinal cord has only a minimal capacity to regenerate (ie, recover), damage to PNS-derived axons often is more apparent in the spinal cord, especially in the relatively large dorsal columns in the cranial cervical region

Distribution of Spinal Tract Lesions

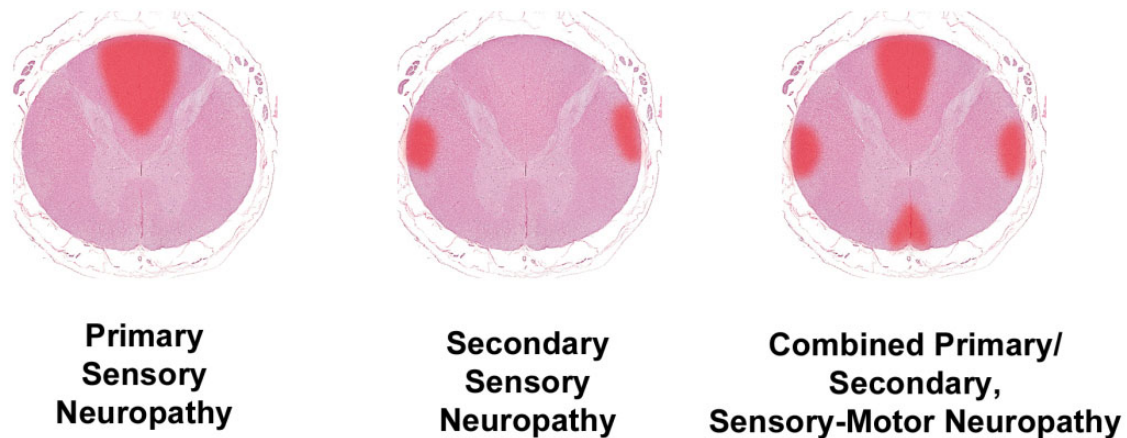


Figure 69. Patterns of spinal cord damage due to peripheral neuropathy in vertebrates with a well-developed neocortex. The schematics demonstrate nerve fiber lesions in white matter tracts (red foci) with respect to spinal cord anatomy in the cranial cervical cord (C₁-C₂), which is the level with the largest contribution of sensory and motor fibers dedicated to PNS functions. *Primary sensory neuropathy* features axonal degeneration in the dorsal funiculi (gracile and cuneate fasciculi). *Secondary sensory neuropathy* yields lesions in the dorsolateral tracts (ie, spinocerebellar fibers). In *combined primary and secondary sensory and motor neuropathy*, lesions occur in the dorsal funiculi, dorsolateral tracts (containing spinocerebellar fibers and crossed pyramidal fibers), and ventromedial tracts (ie, uncrossed pyramidal fibers). In animals lacking a well-developed cerebral cortex, like the chicken, the spinocerebellar fibers are most indicative of peripheral neuropathy. Note: This tract-oriented pattern of spinal cord damage is characteristic for lesions resulting from axonal damage. In contrast, pure demyelinating lesions generally are distributed within all spinal cord columns. PNS indicates peripheral nervous system.

that harbor all the sensory axons arising directly from the forelimb and hind limb.

Summary

This atlas illustrates many key characteristics of normal PNS cell and tissue microanatomy, procedural and processing artifacts, spontaneous PNS background findings, and test article-induced PNS neurotoxic lesions. Familiarity with these features is essential in performing a proficient neuropathology analysis and particularly for reaching the correct interpretation of structural changes in PNS tissues of test species in animal toxicity studies. Comparison of these images with similar illustrations in human PNS neuropathology atlases^{72,80-82} will provide toxicologic pathologists with opportunities to hone their diagnostic skills.

Acknowledgments

The authors would like to thank Ms Beth Mahler for her aid in optimizing the quality of many images included in this compilation and Dr Bernard Jortner for contributing with several images and critical review of this manuscript. In addition, Dr Pardo would like to acknowledge her current and former colleagues from Pfizer Inc who have consulted and shared PNS cases during her work in that company, including Drs Christopher Houle, Katherine Biddle, Rick Perry, Stephane Thibault, Katherine Hammerman, Magalie Bouchard, Xavier Palazzi, Ahmed Shoieb, Karrie Brennehan, Michael Mirsky,

Balasubramanian Manickam, Norimitsu Shirai, Katherine Gropp, Magali Guffroy, Karamjeet Pandher, Mark Evans, and Natasha Neef.




Declaration of Conflicting Interests

The author(s) declared no potential, real, or perceived conflicts of interest with respect to the research, authorship, and/or publication of this article.

Funding

The author(s) received no financial support for the research, authorship, and/or publication of this article.

ORCID iD

Ingrid D. Pardo  <https://orcid.org/0000-0002-3517-3804>
 Mark T. Butt  <https://orcid.org/0000-0001-8613-199X>
 Brad Bolon  <https://orcid.org/0000-0002-6065-1492>

References

- Jortner BS. Mechanisms of toxic injury in the peripheral nervous system: neuropathologic considerations. *Toxicol Pathol.* 2000;28(1):54-69.
- Grogan PM, Katz JS. Toxic neuropathies. *Neurol Clin.* 2005;23(2): 377-396.
- Gonzalez-Duarte A, Robinson-Papp J, Simpson DM. Diagnosis and management of HIV-associated neuropathy. *Neurol Clin.* 2008;26(3): 821-832.
- Azhary H, Farooq MU, Bhanushali M, Majid A, Kassab MY. Peripheral neuropathy: differential diagnosis and management. *Am Fam Physician.* 2010;81(7):887-892.

5. Grisold W, Cavaletti G, Windebank AJ. Peripheral neuropathies from chemotherapeutics and targeted agents: diagnosis, treatment, and prevention. *Neuro-oncology*. 2012;14(Suppl 4):iv45-iv54.
6. Jimenez-Andrade JM, Peters CM, Mejia NA, Ghilardi JR, Kuskowski MA, Mantyh PW. Sensory neurons and their supporting cells located in the trigeminal, thoracic and lumbar ganglia differentially express markers of injury following intravenous administration of paclitaxel in the rat. *Neurosci Lett*. 2006;405(1-2):62-67.
7. Podratz JL, Kulkarni A, Pleticha J, et al. Neurotoxicity to DRG neurons varies between rodent strains treated with cisplatin and bortezomib. *J Neurol Sci*. 2016;362:131-135.
8. Bolon B, Krinke G, Butt MT, et al. STP Position Paper: recommended best practices for sampling, processing, and analysis of the peripheral nervous system (nerves and somatic and autonomic ganglia) during nonclinical toxicity studies. *Toxicol Pathol*. 2018;46(4):372-402.
9. de Lahunta A, Glass E. *Veterinary Neuroanatomy and Clinical Neurology*. 3rd ed. St Louis, MO: Saunders (Elsevier); 2009.
10. Furness JB. Structure of the enteric nervous system. In: *The Enteric Nervous System*. 1st ed. Malden, MA: Blackwell; 2006:1-28.
11. Zochodne DW, Ho LT. Unique microvascular characteristics of the dorsal root ganglion in the rat. *Brain Res*. 1991;559(1):89-93.
12. Sapunar D, Kostic S, Banozic A, Puljak L. Dorsal root ganglion—a potential new therapeutic target for neuropathic pain. *J Pain Res*. 2012;5:31-38.
13. Rigaud M, Gemes G, Barabas ME, et al. Species and strain differences in rodent sciatic nerve anatomy: implications for studies of neuropathic pain. *Pain*. 2008;136(1-2):188-201.
14. Howroyd P. Dissection of the trigeminal ganglion of non-rodent species used in toxicology studies. *Toxicol Pathol*. 2020;48(2).
15. Espinosa-Medina I, Saha O, Boismoreau F, et al. The sacral autonomic outflow is sympathetic. *Science*. 2016;354(6314):893-897.
16. Getty R. *Sisson and Grossman's The Anatomy of the Domestic Animals*. 5th ed. Philadelphia, PA: W. B. Saunders; 1975.
17. Evans HE. *Miller's Anatomy of the Dog*. 3rd ed. Philadelphia, PA: Saunders (Elsevier); 1993.
18. Clarkson C, Brown A, Ekenstedt K, Fletcher TF. *Carnivore Dissection, Lab12: Thoracic cavity: Autonomic nerves and heart; 2015*. <http://vanat.cvm.umn.edu/carnLabs/Lab12/Lab12.html>. Accessed July 25, 2019.
19. Hanani M. Satellite glial cells in sensory ganglia: from form to function. *Brain Res Brain Res Rev*. 2005;48(3):457-476.
20. Hanani M. Satellite glial cells in sympathetic and parasympathetic ganglia: in search of function. *Brain Res Rev*. 2010;64(2):304-327.
21. Andres KH. Untersuchungen über den Feinbau von Spinalganglien (Studies on the fine structure of dorsal root ganglia). *Z Zellforsch*. 1961;55(1):1-48.
22. Miller KE, Richards BA, Kriebel RM. Glutamine-, glutamine synthetase-, glutamate dehydrogenase- and pyruvate carboxylase-immunoreactivities in the rat dorsal root ganglion and peripheral nerve. *Brain Res*. 2002;945(2):202-211.
23. Xie RG, Chu WG, Hu SJ, Luo C. Characterization of different types of excitability in large somatosensory neurons and its plastic changes in pathological pain states. *Intl J Mol Sci*. 2018;19(1):pii: E161. doi: 10.3390/ijms19010161.
24. Snyder JM, Hagan CE, Bolon B, Keene CD. Nervous system. In: Treuting PM, Dintzis SM, Montine KS, eds. *Comparative Anatomy and Histology: A Mouse, Rat, and Human Atlas*. 2nd ed. San Diego, CA: Academic Press (Elsevier); 2018:403-444.
25. Young B, Heath J. *Wheater's Functional Histology: A Text and Colour Atlas*. Edinburgh, Scotland: Elsevier; 2002.
26. Banks R. The muscle spindle. In: Dyck P, Thomas P, eds. *Peripheral Neuropathy*. Vol 1. Philadelphia, PA: Elsevier Saunders; 2005:131-150.
27. Smith KR Jr. The structure and function of the Haarscheibe. *J Comp Neurol*. 1967;131(4):459-474.
28. Smith KR Jr. The ultrastructure of the human Haarscheibe and Merkel cell. *J Invest Dermatol*. 1970;54(2):150-159.
29. Krinke GJ. Neuropathological analysis of the peripheral nervous system. In: Bolon B, Butt MT, eds. *Fundamental Neuropathology for Pathologists and Toxicologists: Principles and Techniques*. Hoboken, NJ: John Wiley & Sons; 2011:365-384.
30. Kiernan JA, Raajakumar N. *Barr's The Human Nervous System: An Anatomical Viewpoint*. 10th ed. Baltimore, MD: Lippincott, Williams and Wilkins; 2014.
31. Yamate J. Integumentary System. 19. The skin and subcutis. In: Suttie AW, Leininger JR, Bradley AE, eds. *Boorman's Pathology of the Rat. Reference and Atlas*. 2nd ed. London, England: Academic Press (Elsevier); 2018:323-346.
32. Krinke G, Heid J, Bittiger H, Hess R. Sensory denervation of the plantar lumbrical muscle spindles in pyridoxine neuropathy. *Acta Neuropathol*. 1978;43(3):213-216.
33. Jirmanová I. Pacinian corpuscles in rats with carbon disulphide neuropathy. *Acta Neuropathol*. 1987;72(4):341-348.
34. Jortner BS. Preparation and analysis of the peripheral nervous system. *Toxicol Pathol*. 2011;39(1):66-72.
35. Butt M, Cramer S, Hodge D. Sampling and evaluating the peripheral portion of the nervous system. *Toxicol Pathol*. 2020;48(2).
36. Fortin JS, Chlipala EA, Shaw DP, Bolon B. Methods optimization for routine sciatic nerve processing in general toxicity studies. *Toxicol Pathol*. 2020;48(2).
37. Carrier CA, Donnelly KB. Post-injection sciatic neuropathy in a cynomolgus macaque (*Macaca fascicularis*). *J Med Primatol*. 2014;43(1):52-54.
38. Bangari DS, Pardo ID, Sellers R, Johnson JA, Ryan S, Thurberg BL. Peripheral nerve microscopic changes related to study procedures: two nonclinical case studies. *Toxicol Pathol*. 2020;48(2).
39. Petrovsky N. Comparative safety of vaccine adjuvants: a summary of current evidence and future needs. *Drug Safety*. 2015;38(11):1059-1074.
40. Cammermeyer J. The importance of avoiding "dark" neurons in experimental neuropathology. *Acta Neuropathologica*. 1961;1(3):245-270.
41. Cammermeyer J. Ischemic neuronal disease of Spielmeyer—a reevaluation. *Arch Neurol*. 1973;29(6):391-393.
42. Garman RH. Common histological artifacts in nervous system tissues. In: Bolon B, Butt MT, eds. *Fundamental Neuropathology for Pathologists and Toxicologists: Principles and Techniques*. Hoboken, NJ: John Wiley & Sons; 2011:191-201.
43. Jortner BS. The return of the dark neuron. A histological artifact complicating contemporary neurotoxicologic evaluation. *Neurotoxicology*. 2006;27(4):628-634. [See comment in *Neurotoxicology* 27: 1126, 2006.]
44. Ebels EJ. Dark neurons, a significant artifact: the influence of the maturational state of neurons on the occurrence of the phenomenon. *Acta Neuropathol*. 1975;33(3):271-273.
45. Krinke GJ, Landes C. The dorsal fascia dentata as a probe of fixation quality in the rodent brain. *Cesk Patol*. 1995;31(1):28-30.
46. Stumm G, Geissel H, Wenzel J, Mennel HD. Early and late morphological effects of experimental HPNS—animal model of psychosis? *Exp Toxicol Pathol*. 2001;53(1):45-55.
47. Levy DE, Brierley JB, Silverman DG, Plum F. Brief hypoxia-ischemia initially damages cerebral neurons. *Arch Neurol*. 1975;32(7):450-456.
48. Kirino T, Sano K. Selective vulnerability in the gerbil hippocampus following transient ischemia. *Acta Neuropathol*. 1984;62(3):201-208.
49. Ohtsuka A, Murakami T. Dark neurons in the mouse brain: an investigation into the possible significance of their variable appearance within a day and their relation to negatively charged cell coats. *Arch Histol Cytol*. 1996;59(1):79-85.
50. Mennel HD, El-Abhar H, Schilling M, Bausch J, Kriegelstein J. Morphology of tissue damage caused by permanent occlusion of middle cerebral artery in mice. *Exp Toxicol Pathol*. 2000;52(5):395-404.
51. Atillo A, Soderfeldt B, Kalimo H, Olsson Y, Siesjö BK. Pathogenesis of brain lesions caused by experimental epilepsy. Light- and electron-microscopic changes in the rat hippocampus following bicuculline-induced status epilepticus. *Acta Neuropathol*. 1983;59(1):11-24.
52. Evans M, Griffiths T, Meldrum B. Early changes in the rat hippocampus following seizures induced by bicuculline or L-allylglycine: a light and electron microscope study. *Neuropathol Appl Neurobiol*. 1983;9(1):39-52.

53. Purpura DP, Gonzalez-Monteagudo O. Acute effects of methoxyppyridoxine on hippocampal end-blade neurons: an experimental study of "special pathoclisis" in the cerebral cortex. *J Neuropathol Exp Neurol*. 1960;19(3):421-432.
54. Rogers-Cotrone T, Burgess MP, Hancock SH, et al. Vacuolation of sensory ganglion neuron cytoplasm in rats with long-term exposure to organophosphates. *Toxicol Pathol*. 2010;38(4):554-559.
55. Krinke GJ. Neuronal vacuolation. *Toxicol Pathol*. 2011;39(7):1140.
56. Krinke GJ, Herrmann A, Korner A, Landes C, Sauner F. Experience with examination of the spinal cord and peripheral nervous system (PNS) in mice: a brief overview. *Exp Toxicol Pathol*. 2014;66(7):277-280.
57. Butt MT. Vacuoles in dorsal root ganglia neurons: some questions. *Toxicol Pathol*. 2010;38(6):999.
58. Butt MT, Sills R, Bradley A. Nervous system. In: Sahota PS, Popp JA, Hardisty JF, Gopinath C, eds. *Toxicologic Pathology: Nonclinical Safety Assessment*. 1st ed. Boca Raton, FL: CRC Press (Taylor & Francis); 2013:895-930.
59. Butt M, Fuji R, Reichelt M, Sharma A, Cramer S. Autophagy of sensory neurons in the trigeminal and dorsal root ganglia of cynomolgus monkeys (*Macaca fascicularis*). *Toxicol Pathol*. 2020;48(2).
60. Rath-Wolfson L, Shvero A, Bubis G, et al. Morphological changes in periprosthetic sympathetic ganglion cells in aging males. *Mol Clin Oncol*. 2017;6(5):713-717.
61. Cotard-Bartley MP, Secchi J, Glomot R, Cavanagh JB. Spontaneous degenerative lesions of peripheral nerves in aging rats. *Vet Pathol*. 1981;18(1):110-113.
62. Eisenbrandt DL, Mattsson JL, Albee RR, Spencer PJ, Johnson KA. Spontaneous lesions in subchronic neurotoxicity testing of rats. *Toxicol Pathol*. 1990;18(1 pt 2):154-164.
63. Blankenship B, Eighmy JJ, Hoffmann G, Schroeder M, Sharma AK, Sorden SD. Findings in historical control Harlan RCCHan:WIST rats from 104-week oral gavage studies. *Toxicol Pathol*. 2016;44(7):947-961.
64. Namgung U. The role of Schwann cell-axon interaction in peripheral nerve regeneration. *Cells Tissues Organs*. 2014;200(1):6-12.
65. Elcock LE, Stuart BP, Hoss HE, et al. Renaut bodies in the sciatic nerve of Beagle dogs. *Exp Toxicol Pathol*. 2001;53(1):19-24.
66. Weber K, Weber F, Longo M, et al. Case report: canine strain- and study condition-dependent formation of Renaut bodies in sciatic nerves of beagle dogs. *Toxicol Pathol*. 2020;48(2).
67. Weber K, Garman RH, Germann PG, et al. Classification of neural tumors in laboratory rodents, emphasizing the rat. *Toxicol Pathol*. 2011;39(1):129-151.
68. Krinke GJ. Nonneoplastic and neoplastic changes in the peripheral nervous system. In: Mohr U, Dungworth DL, Capen CC, eds. *Pathobiology of the Aging Rat*. Vol. 2. Washington, DC: ILSI Press; 1994:83-93.
69. Krinke G. Nonneoplastic and neoplastic lesions of the peripheral nervous system. In: Mohr U, Dungworth DL, Capen CC, Carlton WW, Sundberg JP, Ward JM, eds. *Pathobiology of the Aging Mouse*. Vol 2. Washington, DC: ILSI Press; 1996:83-93.
70. Krinke GJ, Ehrensperger F, Vandeveld M. Non-neoplastic and neoplastic lesions in the peripheral nervous system. In: Mohr U, Carlton WW, Dungworth DL, Benjamin SA, Capen CC, Hahn FF, eds. *Pathobiology of the Aging Dog*. Vol 2. Ames, IA: Iowa State University Press; 2001:10-21.
71. Kaufmann W, Bolon B, Bradley A, et al. Non-proliferative and proliferative lesions of the rat and mouse central and peripheral nervous systems. *Toxicol Pathol*. 2012;40(4 Suppl):87S-157S.
72. Oh SJ. *Color Atlas of Nerve Biopsy Pathology*. Boca Raton, FL: CRC Press; 2002.
73. Dyck PJ, Thomas PK, eds. *Peripheral Neuropathy*. 4th ed. Philadelphia, PA: Elsevier Saunders; 2005.
74. Koelsch B, van den Berg L, Fischer C, Winzen-Reichert B, Kutritz A, Kindler-Rohrborn A. Chemically induced oncogenesis in the peripheral nervous system is suppressed in congenic BDIX.BDIV-Mss1 and -Mss7 rats. *Genes Genomes Genet*. 2015;6(1):59-65.
75. Jortner BS, Shell L, el-Fawal H, Ehrlich M. Myelinated nerve fiber regeneration following organophosphorus ester-induced delayed neuropathy. *Neurotoxicology*. 1989;10(4):717-726.
76. Muratori L, Ronchi G, Raimondo S, Giacobini-Robecchi MG, Fornaro M, Geuna S. Can regenerated nerve fibers return to normal size? A long-term post-traumatic study of the rat median nerve crush injury model. *Microsurgery*. 2012;32(5):383-387.
77. Morfini GA, Burns MR, Stenoien DL, Brady ST. Axonal transport. In: Brady S, Siegel GJ, Albers RW, Price D, eds. *Basic Neurochemistry: Principles of Molecular, Cellular, and Medical Neurobiology*. 8th ed. Waltham, MA: Academic Press (Elsevier); 2012:146-164.
78. Ronchi G, Jager SB, Vaegter CB, Raimondo S, Giacobini-Robecchi MG, Geuna S. Discrepancies in quantitative assessment of normal and regenerated peripheral nerve fibers between light and electron microscopy. *J Periph Nerv Sys*. 2014;19(3):224-233.
79. Bolon B, Garman RH, Pardo ID, et al. STP Position Paper: recommended practices for sampling and processing the nervous system (brain, spinal cord, nerve, and eye) during nonclinical general toxicity studies. *Toxicol Pathol*. 2013;41(7):1028-1048.
80. King R. *Atlas of Peripheral Nerve Pathology*. London, England: Arnold; 1999.
81. Dyck PJ. Pathologic alterations of nerves. In: Dyck PJ, Thomas PK, eds. *Peripheral Neuropathy*. 4th ed. Philadelphia, PA: Saunders (Elsevier); 2005:733-829.
82. Bilbao JM, Schmidt RE. *Biopsy Diagnosis of Peripheral Neuropathy*. 2nd ed. New York, NY: Springer; 2015.